Synthesis, Structures, and Coordinating Properties of Phosphole-Containing Hybrid Calixpyrroles

Takashi Nakabuchi,[†] Yoshihiro Matano,*[,†] and Hiroshi Imahori[†,‡,§]

Department of Molecular Engineering, Graduate School of Engineering, Kyoto University, Nishikyo-ku, Kyoto 615-8510, Japan, Institute for Integrated Cell-Material Sciences, Kyoto University, Nishikyo-ku, Kyoto 615-8510, Japan, and Fukui Institute for Fundamental Chemistry, Kyoto University, 34-4, Takano-Nishihiraki-cho, Sakyo-ku, Kyoto 606-8103, Japan

Received February 4, 2008

Symmetric and asymmetric hybrid calixpyrroles containing a σ^4-phosphole or σ^4-2,3-dihydrophosphole unit (symmetric and asymmetric σ^4-P,N_2,X-hybrids: X = S, O) were prepared by using acid-promoted condensation reactions of the corresponding σ^4-phosphatripyrranes with 2,5-bis(1-hydroxy-1-methylethyl)heteroles. The X-ray crystallographic analyses of the symmetric and asymmetric σ^4-P,N_2,X-hybrids show that the cavity sizes of the σ^4-P,N_2,S-hybrids are larger than those of the σ^4-P,N_2,O-hybrids, mainly reflecting the difference in edge-to-edge distances of the thiophene and furan rings. The symmetric σ^4-P,N_2,X-hybrids and the asymmetric σ^4-P,N_2,S-hybrid were successfully converted to the corresponding σ^3 forms by reductive desulfurization at the phosphorus center. Each of the symmetric σ^3-P,N_2,X-hybrids was obtained as a mixture of two conformers, where the lone pair of the phosphorus atom is located inside (*in*) and outside (*out*) the cavity. The interconversion between the *in* and *out* type conformers of the asymmetric σ^3-P,N_2,S-hybrid was sufficiently slow to isolate each of them. The complexation reactions of the symmetric σ^3-P,N_2,S-hybrid with Au(I), Pt(II), and Pd(II) ions afforded both of the *in* and *out* type complexes, where the *in* type complexes were the thermodynamically favored products. In the complexation reactions of the asymmetric σ^3-P,N_2,S-hybrids, the stereochemistry at the phosphorus center was retained to give the *in* or *out* type complex exclusively. In the *in-in* type *trans*-M(II)-bis(phosphine) complexes (M = Pt, Pd) derived from the symmetric and asymmetric σ^3-P,N_2,S-hybrids, the M−Cl fragment is bound above the cavities of the two macrocycles. The crystal structures and the ^{1}H NMR spectra of these M(II) complexes reveal that the P,N_2,S-hybrid calixpyrroles bind the M−Cl fragments through P−M coordination and cooperative NH−Cl hydrogen-bonding interactions.

Introduction

Calix[4]pyrroles,[1,2] which are regarded as the pyrrole analogue of calix[4]arenes, have attracted growing interest in supramolecular chemistry, since the discovery by Sessler and co-workers that these macrocycles can bind anionic[3] and neutral[4] species by utilizing the pyrrole-NH groups as the multiple hydrogen-bonding donors, while Floriani and co-workers extensively studied the coordination chemistry of calix[4]pyrroles, in which these macrocycles had been used as fully deprotonated, tetraanionic N_4 ligands for various metals.[5] Inspired by these pioneering studies, many research groups have designed and

* To whom correspondence should be addressed. E-mail: matano@scl.kyoto-u.ac.jp. Tel: +81-75-383-2567. Fax: +81-75-383-2571.

† Department of Molecular Engineering.

‡ Institute for Integrated Cell-Material Sciences.

§ Fukui Institute for Fundamental Chemistry.

(1) Baeyer, A. *Ber. Dtsch. Chem. Ges.* **1886**, *19*, 2184.

(2) For reviews, see: (a) Gale, P. A.; Sessler, J. L.; Král, V. *Chem. Commun.* **1998**, 1. (b) Floriani, C.; Floriani-Moro, R. In *The Porphyrin Handbook*; Kadish, K. M., Smith, K. M., Guilard, R., Eds.; Academic Press: San Diego, CA, 2000; Vol. 3, pp 385−403. (c) Sessler, J. L.; Gale, P. A. In *The Porphyrin Handbook*; Kadish, K. M., Smith, K. M., Guilard, R., Eds.; Academic Press: San Diego, CA, 2000; Vol *6*, pp 257−278. (d) Gale, P. A.; Anzenbacher, P., Jr.; Sessler, J. L. *Coord. Chem. Rev.* **2001**, *222*, 57.

(3) For example, see: (a) Gale, P. A.; Sessler, J. L.; Král, V.; Lynch, V. *J. Am. Chem. Soc.* **1996**, *118*, 5140. (b) Miyaji, H.; Anzenbacher, P., Jr.; Sessler, J. L.; Bleasdale, E. R.; Gale, P. A. *Chem. Commun.* **1999**, 1723. (c) Anzenbacher, P., Jr.; Jursíková, K.; Sessler, J. L. *J. Am. Chem. Soc.* **2000**, *122*, 9350. (d) Anzenbacher, P., Jr.; Try, A. C.; Miyaji, H.; Jursíková, K.; Lynch, V. M.; Marquez, M.; Sessler, J. L. *J. Am. Chem. Soc.* **2000**, *122*, 10268. (e) Woods, C. J.; Camiolo, S.; Light, M. E.; Coles, S. J.; Hursthouse, M. B.; King, M. A.; Gale, P. A.; Essex, J. W. *J. Am. Chem. Soc.* **2002**, *124*, 8644. (f) Lee, C.-H.; Na, H.-K.; Yoon, D.-W.; Won, D.-H.; Cho, W.-S.; Lynch, V. M.; Shevchuk, S. V.; Sessler, J. L. *J. Am. Chem. Soc.* **2003**, *125*, 7301. (g) Nishiyabu, R.; Anzenbacher, P., Jr. *J. Am. Chem. Soc.* **2005**, *127*, 8270. (h) Miyaji, H.; Kim, H.-K.; Sim, E.-K.; Lee, C.-K.; Cho, W.-S.; Sessler, J. L.; Lee, C.-H. *J. Am. Chem. Soc.* **2005**, *127*, 12510.

(4) Allen, W. E.; Gale, P. A.; Brown, C. T.; Lynch, V. M.; Sessler, J. L. *J. Am. Chem. Soc.* **1996**, *118*, 12471.

(5) For example, see: (a) Jacoby, D.; Floriani, C.; Chiesi-Villa, A.; Rizzoli, C. *J. Chem. Soc., Chem. Commun.* **1991**, 220. (b) Jacoby, D.; Floriani, C.; Chiesi-Villa, A.; Rizzoli, C. *J. Chem. Soc., Chem. Commun.* **1991**, 790. (c) Jubb, J.; Floriani, C.; Chiesi-Villa, A.; Rizzoli, C. *J. Am. Chem. Soc.* **1992**, *114*, 6571. (d) Jacoby, D.; Floriani, C.; Chiesi-Villa, A.; Rizzoli, C. *J. Am. Chem. Soc.* **1993**, *115*, 7025. (e) Kretz, C. M.; Gallo, E.; Solari, E.; Floriani, C.; Chiesi-Villa, A.; Rizzoli, C. *J. Am. Chem. Soc.* **1994**, *116*, 10775. (f) Piarulli, U.; Solari, E.; Floriani, C.; Chiesi-Villa, A.; Rizzoli, C. *J. Am. Chem. Soc.* **1996**, *118*, 3634. (g) Floriani, C.; Solari, E.; Solari, G.; Chiesi-Villa, A.; Rizzoli, C. *Angew. Chem., Int. Ed.* **1998**, *37*, 2245. (h) Bonomo, L.; Solari, E.; Floriani, C.; Chiesi-Villa, A.; Rizzoli, C. *J. Am. Chem. Soc.* **1998**, *120*, 12972. (i) Bonomo, L.; Dandin, O.; Solari, E.; Floriani, C.; Scopelliti, R. *Angew. Chem., Int. Ed.* **1999**, *38*, 913. (j) Bonomo, L.; Solari, E.; Latronico, M.; Scopelliti, R.; Floriani, C. *Chem.−Eur. J.* **1999**, *5*, 2040.

(6) (a) Arumugam, N.; Jang, Y.-S.; Lee, C.-H. *Org. Lett.* **2000**, *2*, 3115. (b) Cafeo, G.; Kohnke, F. H.; La Torre, G. L.; Parisi, M. F.; Nascone, R. P.; White, A. J. P.; Williams, D. J. *Chem.−Eur. J.* **2002**, *8*, 3148. (c) Nagarajan, A.; Ka, J.-W.; Lee, C.-H. *Tetrahedron* **2001**, *57*, 7323. (d) Lee, E.-C.; Park, Y.-K.; Kim, J.-H.; Hwang, H.; Kim, Y.-R.; Lee, C.-H. *Tetrahedron Lett.* **2002**, *43*, 9493. (e) Song, M.-Y.; Na, H.-K.; Kim, E.-Y.; Lee, S.-J.; Kim, K.-I.; Baek, E.-M.; Kim, H.-S.; An, D. K.; Lee, C.-H. *Tetrahedron Lett.* **2004**, *45*, 299. (f) Sessler, J. L.; An, D.; Cho, W.-S.; Lynch, V.; Yoon, D.-W.; Hong, S.-J.; Lee, C.-H. *J. Org. Chem.* **2005**, *70*, 1511.

10.1021/om800099h CCC: $40.75
Publication on Web 05/28/2008

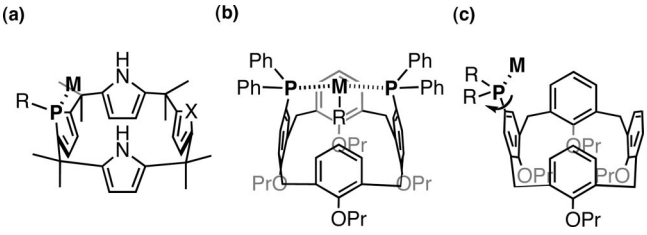

Figure 1. Schematic views of metal complexes of the phosphole-containing hybrid calixpyrroles (a) and P(III)-functionalized calix[4]arenes (b, c).

prepared a wide variety of hybrid calixpyrroles containing nonpyrrolic arene units such as furan,[6] thiophene,[6c–f] pyridine,[7,8] and benzene[8] to modify the binding ability of the calixpyrrole platform. To our knowledge, however, no attempt has been made to incorporate phosphole into the calixpyrrole platform,[9–11] despite its utility as neutral P ligand for transition metals.[12] We expected that phosphole-containing hybrid calixpyrroles, formally obtained by incorporating a phosphole unit into the macrocyclic framework of the calixpyrrole, would exhibit some promising features as the structurally well-defined macrocyclic P ligands while keeping the hosting function (Figure 1a).

The coordination chemistry of the calix[4]arene derivatives bearing P(III) functionalities[13] at the upper[14] or lower rims[15] has already been studied by several groups. For example, Matt and co-workers used an upper-rim bis(phosphine)-functionalized calix[4]arene as a bidentate P ligand for Pt(II), Pd(II), and Ru(II) complexes, in which the M−R fragments were entrapped inside the macrocyclic cavity through *trans*-P−M−P chelation (Figure 1b).[14d] The phosphole-containing hybrid calixpyrroles are distinct from the P(III)-functionalized calix[4]arenes in three aspects. First, as seen in the supramolecular chemistry of the parent calix[4]pyrroles, the macrocyclic platform of the phosphole-containing hybrid calixpyrroles provides multiple hydrogen-bonding sites for negatively charged groups. Second, the size, shape, and binding ability of the hybrid platform are tunable by altering the combination of the heterole components (e.g., X in Figure 1a). Finally, the rigidity of the phosphole unit allows the coordinated metal to be located above the cavity without chelation, which is difficult for the mono-P(III)-functionalized calix[4]arenes owing to the C(calix)−P bond rotation (Figure 1c).[14g,h]

Chart 1. Structures of Phosphole-Containing Hybrid Calixpyrroles 1S and 2S

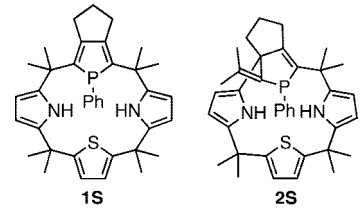

Here we report the synthesis, structures, and coordination behavior of the hybrid calixpyrroles **1S** and **2S** (Chart 1), which contain a phosphole unit and a 2,3-dihydrophosphole unit, respectively, as one of the heterocyclic components. The structures and thermal stabilities of the Au(I), Pt(II), and Pd(II)

(7) (a) Jacoby, D.; Isoz, S.; Floriani, C.; Chiesi-Villa, A.; Rizzoli, C. *J. Am. Chem. Soc.* **1995**, *117*, 2793. (b) Král, V.; Gale, P. A.; Anzenbacher, P., Jr.; Jursíková, K.; Lynch, V.; Sessler, J. L. *Chem. Commun.* **1998**, 9.

(8) Sessler, J. L.; Cho, W,-S.; Lynch, V.; Král, V. *Chem.−Eur. J.* **2002**, *8*, 1134.

(9) For reviews of phosphole, see: (a) Mathey, F. *Chem. Rev.* **1988**, *88*, 429. (b) Quin, L. D. In *Comprehensive Heterocyclic Chemistry*; Katritzky, A. R., Rees, C. W., Scriven, E. F. V., Eds.; Elsevier: Oxford, 1996; Vol. 2. (c) Hissler, M.; Dyer, P. W.; Réau, R. *Coord. Chem. Rev.* **2003**, *244*, 1. (d) Mathey, F. *Angew. Chem., Int. Ed.* **2003**, *42*, 1578. (e) Baumgartner, T.; Réau, R. *Chem. Rev.* **2006**, *106,* 468; Correction: **2007**, *107*, 303.

(10) Recently we reported related phosphole-containing porphyrinoids: (a) Matano, Y.; Miyajima, T.; Nakabuchi, T.; Imahori, H.; Ochi, N.; Sakaki, S. *J. Am. Chem. Soc.* **2006**, *128*, 11760. (b) Matano, Y.; Nakabuchi, T.; Miyajima, T.; Imahori, H.; Nakano, H. *Org. Lett.* **2006**, *8*, 5713. (c) Matano, Y.; Miyajima, T.; Ochi, N.; Nakabuchi, T.; Shiro, M.; Nakao, Y.; Sakaki, S.; Imahori, H. *J. Am. Chem. Soc.* **2008**, *130*, 990. (d) Matano, Y.; Nakashima, M.; Nakabuchi, T.; Imahori, H.; Fujishige, S.; Nakano, H. *Org. Lett.* **2008**, *10*, 553.

(11) Mathey and co-workers prepared some phosphole-containing macrocycles: (a) Mathey, F.; Mercier, F.; Nief, F.; Fischer, J.; Mitschler, A. *J. Am. Chem. Soc.* **1982**, *104*, 2077. (b) Laporte, F.; Mercier, F.; Ricard, L.; Mathey, F. *J. Am. Chem. Soc.* **1994**, *116*, 3306. (c) Deschamps, E.; Ricard, L.; Mathey, F. *J. Chem. Soc., Chem. Commun.* **1995**, 1561. (d) Mercier, F.; Laporte, F.; Ricard, L.; Mathey, F.; Schröder, M.; Regitz, M. *Angew. Chem., Int. Ed. Engl.* **1997**, *36*, 2364. (e) Duan, Z.; Clochard, M.; Donnadieu, B.; Mathey, F.; Tham, F. S. *Organometallics* **2007**, *26*, 3617.

(12) For example, see: (a) Macdugall, J. J.; Nelson, J. H.; Mathey, F.; Mayerle, J. J. *Inorg. Chem.* **1980**, *19*, 709. (b) Herrmann, W. A.; Thiel, W. R.; Priermeier, T.; Herdtweck, E. *J. Organomet. Chem.* **1994**, *481*, 253. (c) Gouygou, M.; Tissot, O.; Daran, J.-C.; Balavoine, G. G. A. *Organometallics* **1997**, *16*, 1008. (d) Csók, Z.; Keglevich, G.; Petocz, G.; Kollár, L. *Inorg. Chem.* **1999**, *38*, 831. (e) Doherty, S.; Eastham, G. R.; Tooze, R. P.; Scanlan, T. H.; Williams, D.; Elsegood, M. R. J.; Clegg, W. *Organometallics* **1999**, *18*, 3558. (f) Doherty, S.; Robins, E. G.; Knight, J. G.; Newman, C. R.; Rhodes, B.; Champkin, P. A.; Clegg, W. *J. Organomet. Chem.* **2001**, *640*, 182. (g) Ogasawara, M.; Yoshida, K.; Hayashi, T. *Organometallics* **2001**, *20*, 1014. (h) Tissot, O.; Gouygou, M.; Dallemer, F.; Daran, J.-C.; Balavoine, G. G. A. *Eur. J. Inorg. Chem.* **2001**, 2385. (i) Sauthier, M.; Leca, F.; Toupet, L.; Réau, R. *Organometallics* **2002**, *21*, 1591. (j) Hydrio, J.; Gouygou, M.; Dallemer, F.; Balavoine, G. G. A.; Daran, J.-C. *J. Organomet. Chem.* **2002**, *643−644*, 19. (k) Hydrio, J.; Gouygou, M.; Dallemer, F.; Daran, J.-C.; Balavoine, G. G. A. *Tetrahedron: Asymmetry* **2002**, *13*, 1097. (l) Thoumazet, C.; Melaimi, M.; Ricard, L.; Mathey, F.; Le Floch, P. *Organometallics* **2003**, *22*, 1580. (m) Thoumazet, C.; Grutzmacher, H.; Deschamps, B.; Ricard, L.; Le Floch, P. *Eur. J. Inorg. Chem.* **2006**, 3911.

(13) Wieser, C.; Dielman, C. B.; Matt, D. *Coord. Chem. Rev.* **1997**, *165*, 93.

(14) For examples of upper-rim functionalization, see: (a) Hamada, F.; Fukugaki, T.; Murai, K.; Orr, G. W.; Atwood, J. L. *J. Inclusion Phenom.* **1991**, *10*, 57. (b) Ozegowski, S.; Costisella, B.; Gloede, J. *Phosphorous, Sulfur, Silicon Relat. Elem.* **1996**, *119*, 209. (c) Gloede, J.; Ozegowski, S.; Köckritz, A.; Keitel, I. *Phosphorous, Sulfur, Silicon Relat. Elem.* **1997**, *131*, 141. (d) Wieser-Jeunesse, C.; Matt, D.; De Cian, A. *Angew. Chem., Int. Ed.* **1998**, *37*, 2861. (e) Bagatin, I. A.; Matt, D.; Thönnessen, H.; Jones, P. G. *Inorg. Chem.* **1999**, *38*, 1585. (f) Shimizu, S.; Shirakawa, S.; Sasaki, Y.; Hirai, C. *Angew. Chem., Int. Ed.* **2000**, *39*, 1256. (g) Vézina, M.; Gagnon, J.; Villeneuve, K.; Drouin, M.; Harvey, P. D. *Chem. Commun.* **2000**, 1073. (h) Vézina, M.; Gagnon, J.; Villeneuve, K.; Drouin, M.; Harvey, P. D. *Organometallics* **2001**, *20*, 273. (i) Takenaka, K.; Obora, Y.; Jiang, L. H.; Tsuji, Y. *Bull. Chem. Soc. Jpn.* **2001**, *74*, 1709. (j) Takenaka, K.; Obora, Y.; Jiang, L. H.; Tsuji, Y. *Organometallics* **2002**, *21*, 1158. (k) Plourde, F.; Gilbert, K.; Gagnon, J.; Harvey, P. D. *Organometallics* **2003**, *22*, 2862.

(15) For examples of lower-rim functionalization, see: (a) Floriani, C.; Jacoby, D.; Chiesi-Villa, A.; Guastini, C. *Angew. Chem., Int. Ed. Engl.* **1989**, *28*, 1376. (b) Khasnis, D. V.; Lattman, M.; Gutsche, C. D. *J. Am. Chem. Soc.* **1990**, *112*, 9422. (c) Moran, J. K.; Roundhill, D. M. *Inorg. Chem.* **1992**, *31*, 4213. (d) Loeber, C.; Matt, D.; De Cian, A.; Fischer, J. *J. Organomet. Chem.* **1994**, *475*, 297. (e) Loeber, C.; Wieser, C.; Matt, D.; De Cian, A.; Fischer, J.; Toupet, L. *Bull. Soc. Chim. Fr.* **1995**, *132*, 166. (f) Cameron, B. R.; van Veggel, F. C. J. M.; Reinhoudt, D. N. *J. Org. Chem.* **1995**, *60*, 2802. (g) Wieser, C.; Matt, D.; Toupet, L.; Bourgeois, H.; Kintzinger, J.-P. *J. Chem. Soc., Dalton Trans.* **1996**, 4041. (h) Stolmár, M.; Floriani, C.; Chiesi-Villa, A.; Rizzoli, C. *Inorg. Chem.* **1997**, *36*, 1694. (i) Faidherbe, P.; Wieser, C.; Matt, D.; Harriman, A.; De Cian, A.; Fischer, J. *Eur. J. Inorg. Chem.* **1998**, 451. (j) Csók, Z.; Szalontai, G.; Czira, G.; Kollár, L. *J. Organomet. Chem.* **1998**, *570*, 23. (k) Paciello, R.; Siggel, l.; Röper, M. *Angew. Chem., Int. Ed.* **1999**, *38*, 1920. (l) Parlevliet, F. J.; Zuideveld, M. A.; Kiener, C.; Kooijman, H.; Spek, A. L.; Kamer, P. C. J.; van Leeuwen, P. W. N. M. *Organometallics* **1999**, *18*, 3394. (m) Cobley, C. J.; Ellis, D. D.; Orpen, A. G.; Pringle, P. G. *J. Chem. Soc., Dalton Trans.* **2000**, 1109. (n) Parlevliet, F. J.; Kiener, C.; Fraanje, J.; Goubitz, K.; Lutz, M.; Spek, A. L.; Kamer, P. C. J.; van Leeuwen, P. W. N. M. *J. Chem. Soc., Dalton Trans.* **2000**, 1113. (o) Dieleman, C.; Steyer, S.; Jeunesse, C.; Matt, D. *J. Chem. Soc., Dalton Trans.* **2001**, 2508.

Scheme 1. Synthesis of the σ^4-P,N_2,S- and σ^4-P,N_2,O-Hybrids

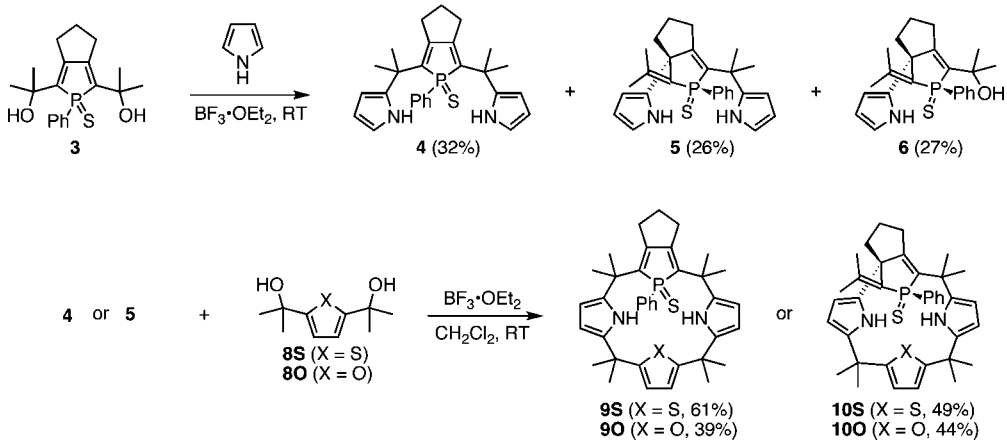

complexes are also reported.[16] As expected, **1S** and **2S** have proven to behave as monodentate P ligands, whose macrocyclic frameworks provide hydrogen-bond-donating NH groups to the Pd−Cl and Pt−Cl fragments.

Results and Discussion

Synthesis of Hybrid Calixpyrroles Containing σ^4-Phosphole or σ^4-2,3-Dihydrophosphole Units. Scheme 1 outlines the synthesis of calix[1]phosphole[1]thiophene[2]pyrroles and calix[1]phosphole[1]furan[2]pyrroles (denoted hereafter as P,N_2,S- and P,N_2,O-hybrids). Treatment of 2,5-bis(1-hydoroxy-1-methylethyl)phosphole *P*-sulfide (**3**)[17] with $BF_3 \cdot OEt_2$ in pyrrole, followed by column chromatography on silica gel, gave an expected condensation product, **4**, in 32% yield together with unexpected products **5** and **6** in 26% and 27% yield, respectively. Presumably, the nonaromatic character of the phosphole ring allows the positive charge of carbenium intermediate **7** to delocalize onto the β-carbons (eq 1).[18,19] The structures of **4**, **5**, and **6** were characterized by standard spectroscopic techniques. Judging from the ^{1}H and ^{31}P NMR spectra, **5** and **6** were obtained as single diastereomers.[20] The BF_3-promoted dehydrative condensation of **4** with 2,5-bis(1-hydroxy-1-methylethyl)thiophene (**8S**)[6c,21] and 2,5-bis(1-hydroxy-1-methylethyl)furan (**8O**)[6c,21] gave symmetric σ^4-P,N_2,X-hybrids **9S** (X = S) and **9O** (X = O) in 61% and 39% yield, respectively. Similar condensations of **5** with **8S** and **8O** afforded the corresponding asymmetric σ^4-P,N_2,X-hybrids **10S** and **10O** in moderate yields. Compounds **9S**, **9O**, **10S**, and **10O** were characterized by spectroscopic methods. In their mass spectra, parent ion peaks were observed at *m*/*z* 610 (for **9S** and **10S**) and *m*/*z* 595 (for **9O** and **10O**), attributable to the 1:1 condensation products. In the ^{31}P NMR spectra of **9S**, **9O**, **10S**, and **10O**, only one peak was observed at δ 69.6, 69.4, 62.3, and 63.1 ppm, respectively, indicating that a single diastereomer had been isolated in each reaction. In the ^{1}H NMR spectra in $CDCl_3$, the NH protons appeared considerably downfield (δ 7.84−9.32 ppm) relative to those of the σ^3 type compounds **1S**, **1O**, and **2S** (δ 6.4−7.57 ppm), implying that the hydrogen-bonding interaction was present in solution (*vide infra*).

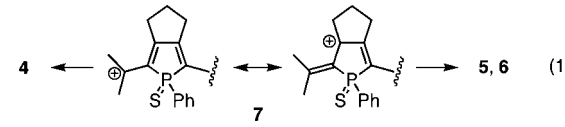

Crystal Structures of σ^4-Hybrids. Crystal structures of **9S**, **9O**, **10S**, and **10O** were elucidated by X-ray crystallography. The ORTEP diagrams of **9S** and **10S** are shown in Figures 2 and 3, and those of **9O** and **10O** are shown in Figures S1 and S2 (Supporting Information). The crystallographic parameters are summarized in Table S1 (Supporting Information). In the symmetric hybrids **9S** and **9O**, the pyrrole rings are connected to the 2- and 5-positions of the phosphole ring through the $-CMe_2-$ bridge. On the other hand, in the asymmetric hybrids

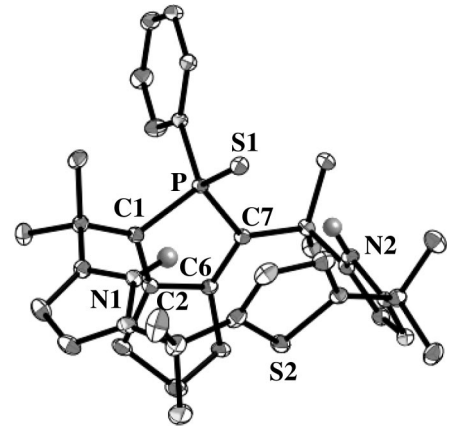

Figure 2. ORTEP diagram of **9S** (30% probability ellipsoids). Except for NH, hydrogen atoms are omitted for clarity. Selected bond lengths and distances (Å): S1−P, 1.9724(5); C1−C2, 1.344(2); C2−C6, 1.485(2); C6−C7, 1.341(2); S1···N1, 3.37; S1···N2, 3.62.

(16) A preliminary communication was published in: Matano, Y.; Nakabuchi, T.; Miyajima, T.; Imahori, H. *Organometallics* **2006**, *25*, 3105.

(17) Matano, Y.; Miyajima, T.; Nakabuchi, T.; Matsutani, Y.; Imahori, H. *J. Org. Chem.* **2006**, *71*, 5792.

(18) Recently, Mathey and co-workers have reported that 2,5-bis(hydroxy(phenyl)methyl)phosphole P-sulfide reacts with a tripyrrane at one of the phosphole-β-positions under Friedel−Crafts conditions to produce a P-confused carbaporphyrinoid, which contains the 2,3-dihydro-3-pyrrolylphosphole subunit like **5** and **6**. See ref 11e.

(19) When **6** was reacted with excess pyrrole for 5 h in the presence of $BF_3 \cdot OEt_2$, **5** was obtained as the main product (ca. 40%) with a substantial recovery of unreacted **6** (ca. 40%). Therefore, **6** is a possible precursor of **5**.

(20) In the ^{1}H NMR spectra, the NH protons of **5** and **6** appeared at the relatively downfield region (δ 7.97−9.46 ppm) comparable to those of **10S** and **10O** (δ 7.84−9.32 ppm), in which all the NH protons are hydrogen-bonded to the P═S moiety of the phosphole ring (*vide infra*). It is therefore likely that the pyrrole groups and the sulfur atom in **5** and **6** are located on the same side of the 2,3-dihydrophosphole ring, similar to those in **10S** and **10O**.

(21) Chadwick, D. J.; Willbe, C. *J. Chem. Soc., Perkin Trans. 1* **1977**, 887.

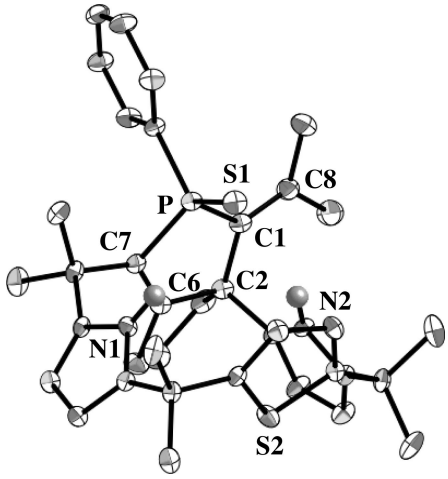

Figure 3. ORTEP diagram of **10S** (50% probability ellipsoids). Except for NH, hydrogen atoms are omitted for clarity. Selected bond lengths and distances (Å): S1−P, 1.9772(14); C1−C2, 1.512(5); C1−C8, 1.334(5); C2−C6, 1.540(5); C6−C7, 1.337(4); S1···N1, 3.60; S1···N2, 3.58.

Table 1. Dihedral Angles and N···S1 Distances

	dihedral angles (deg)[a]			N···S1
compound	phosphole	thiophene/furan	pyrrole	distances (Å)
9S	87.0	71.4	32.0, 56.2	3.37, 3.62
9O	89.8	71.5	32.5, 42.3	3.34, 3.45
10S	87.4	81.1	60.9, 62.9	3.58, 3.60
10O	82.2	88.7	44.3, 47.2	3.58, 3.61

[a] Dihedral angles between the heterole ring and the mean plane of the four (three, in the case of **10S** and **10O**) bridging *meso* carbon atoms.

10S and **10O**, one of the pyrrole rings is directly connected to the 3-position of the 2,3-dihydrophosphole ring, producing two chiral centers at the phosphorus and β-carbon atoms. The P═S sulfur atom and the pyrrole rings are located on the same side, suggesting that the stereochemistry of **5** was retained in the condensation with **8S** and **8O** (*vide supra*).

In the solid state, **9S**, **10S**, and **10O** adopt a partial cone conformation, whereas **9O** adopts a cone conformation. All of the hybrids possess a trapezoid-like cavity, where the P═S moiety is located inside. The phosphole, 2,3-dihydrophosphole, thiophene, and furan rings stand almost perpendicular to a plane formed by the four (**9S** and **9O**) or three (**10S** and **10O**) bridging *meso* carbon atoms, whereas the pyrrole rings are tilted considerably to direct their NH groups toward the sulfur atom of the P═S group (Table 1). The observed N···S1 distances of 3.34−3.62 Å indicate that the hydrogen-bonding interaction is present between the sulfur atom and the NH protons in **9S**, **9O**, **10S**, and **10O**.[22]

As shown in Table 2, the cavity sizes of **9S** and **10S** are larger than those of **9O** and **10O**, mainly reflecting the difference in edge-to-edge distances *b* between the thiophene (**9S**: 5.44 Å and **10S**: 5.40 Å) and furan (**9O**: 4.94 Å and **10O**: 4.91 Å) subunits. These data clearly show that the cavity size of hybrid calixpyrroles is tunable by simply changing the combination of the heterole subunits.

Synthesis of σ^3-Hybrids. In order to prepare the σ^3 type phosphole-containing calixpyrroles, reductive desulfurization of the symmetric σ^4-P,N_2,X-hybrids **9S** and **9O** and asymmetric

Table 2. Edge-to-edge Distances (Å) of 9S, 9O, 10S, and 10O

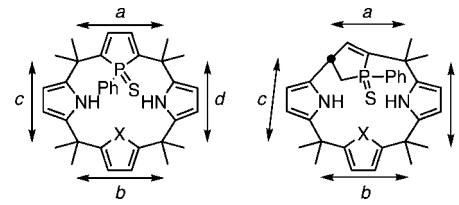

	9S (X = S)	**9O** (X = O)		**10S** (X = S)	**10O** (X = O)
a	5.68	5.67	a^a	3.97	3.96
b	5.44	4.94	*b*	5.40	4.91
c	5.00	5.01	c^a	5.02	5.05
d	5.06	5.03	*d*	5.02	5.06

[a] Defined by the distances between the bridging carbon and the β-carbon atom of the dihydrophosphole unit (indicated by "●").

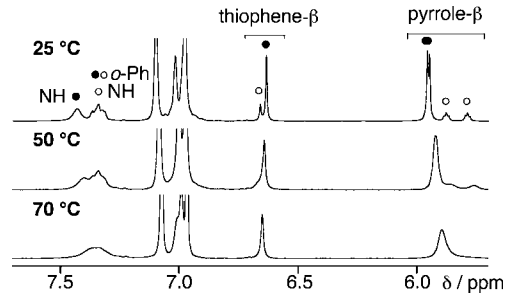

Figure 4. Variable-temperature ^{1}H NMR spectra of **1S** in toluene-d_8. Filled circles: major conformer; open circles: minor conformer.

σ^4-P,N_2,S-hybrid **10S** was examined. When heated with 2.8 equiv of $P(NMe_2)_3$ in refluxing toluene for 33 h, **9S** was completely consumed to afford the symmetric σ^3-P,N_2,S-hybrid **1S** in 92% yield (eq 2). Similarly, **9O** was converted to the symmetric σ^3-P,N_2,O-hybrid **1O** in 72% yield. The ^{1}H and ^{31}P NMR spectra indicate that each of **1S** and **1O** exists as a mixture of two conformers, in which the lone pair of the phosphorus atom is located inside and outside the cavity (**1X**$_{in}$ and **1X**$_{out}$ in eq 3; X = S, O). That is, two sets of ^{1}H resonances and two ^{31}P peaks (δ 31.4 and 32.1 ppm for **1S**; δ 32.3 and 37.6 ppm for **1O**) were observed at 25 °C in toluene-d_8, whereas they coalesced at 70 °C (Figure 4 for **1S**; Figure S3 (Supporting Information) for **1O**). Unfortunately, **1X**$_{in}$ and **1X**$_{out}$ could not be separated at 25 °C, suggesting that interconversion between the two conformers takes place rapidly even at this temperature. It is well known that a pyramidal inversion barrier for phosphole (ca. 16 kcal mol^{-1}) is smaller than those of the conventional triorganylphosphines (30−35 kcal mol^{-1}) due to the aromatic stabilization at the planar transition state.[23] The ratios of major/minor conformers in **1S** and **1O** at 25 °C were determined to be 4:1 and 5:1, respectively, based on the integral values.

In contrast to the desulfurization of the symmetric hybrids, a large excess amount of $P(NMe_2)_3$ (130 equiv) and a longer reaction time (60 h) were needed for the complete conversion of the asymmetric σ^4-P,N_2,S-hybrid **10S** to σ^3-P,N_2,S-hybrid **2S** (eq 4), which was obtained as a mixture of two conformers **2S**$_{in}$ and **2S**$_{out}$. However, the rate of interconversion between **2S**$_{in}$ and **2S**$_{out}$ is so slow at room temperature that both of them could be isolated by column chromatography. The ^{31}P NMR spectra of **2S**$_{in}$ and **2S**$_{out}$ in $CDCl_3$ showed only one peak at δ

(22) The N···S distances for the NH···S hydrogen bonds in silver−antimony sulfides were reported to be 3.20−3.65 Å: Vaqueiro, P.; Chippindale, A. M.; Cowley, A. R.; Powell, A. V. *Inorg. Chem.* **2003**, *42*, 7846.

(23) (a) Egan, W.; Tang, R.; Zon, G.; Mislow, K. *J. Am. Chem. Soc.* **1971**, *93*, 6205. (b) Deschamps, E.; Ricard, L.; Mathey, F. *Angew. Chem., Int. Ed. Engl.* **1994**, *33*, 1158. See also refs 11b,d.

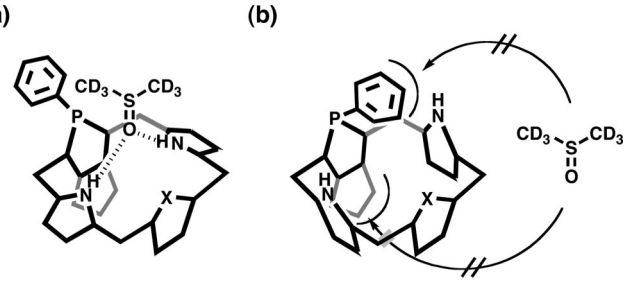

Figure 5. Schematic views of possible interactions of DMSO-d_6 with (a) $\mathbf{1X}_{in}$ and (b) $\mathbf{1X}_{out}$.

29.5 and 17.7 ppm, respectively. The structures of these two conformers were confirmed by X-ray crystallographic analyses of their metal complexes (*vide infra*).

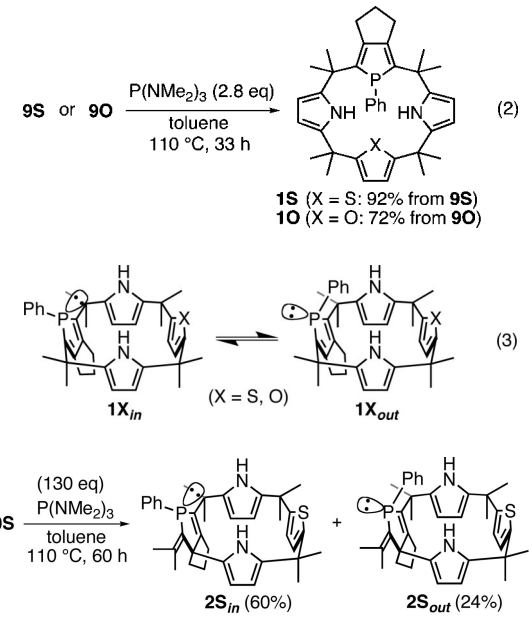

To assign the structures of the major and minor conformers in the symmetric hybrids **1X**, we performed ^{1}H NMR titration measurements of **1X** using dimethyl sulfoxide-d_6 (DMSO-d_6) as a guest, which were originally reported by Sessler and coworkers for evaluating the hydrogen-bonding ability of *meso*-octamethylcalix[4]pyrrole. These authors concluded that the observed downfield shift of the NH protons stems from the multiple hydrogen-bonding interactions between the pyrrolic NH groups and the S-oxo moiety of DMSO.[4] The results of the present system are summarized in Figure S4 (Supporting Information). As the amount of DMSO-d_6 increased, the NH peaks due to the major conformer in **1X** shifted downfield [$\Delta\delta$ = 0.06 ppm (10 equiv), 0.11 ppm (20 equiv) for **1S**;[24] $\Delta\delta$ = 0.09 ppm (10 equiv), 0.17 ppm (20 equiv) for **1O**]. By contrast, the addition of DMSO-d_6 caused no appreciable spectral change for the minor conformer. These observations suggest that the major and minor conformers in toluene-d_8 are $\mathbf{1X}_{in}$ and $\mathbf{1X}_{out}$, respectively. Namely, $\mathbf{1S}_{in}$ and $\mathbf{1O}_{in}$ are likely to bind DMSO-d_6 through the cooperative hydrogen-bonding interaction between two NH protons and the S=O group (Figure 5a,) whereas $\mathbf{1S}_{out}$ and $\mathbf{1O}_{out}$ are unlikely to bind DMSO-d_6 at the core because the phenyl and trimethylene groups would protect the NH groups sterically (Figure 5b). This assignment was strongly supported by the results on similar titration measurements for the isolated asymmetric hybrids $\mathbf{2S}_{in}$ and $\mathbf{2S}_{out}$. On addition of DMSO-d_6 (20 equiv), the NH peaks of $\mathbf{2S}_{in}$ were shifted downfield considerably [$\Delta\delta$ > 0.6 ppm] (Figure S4c), while $\mathbf{2S}_{out}$ displayed negligible spectral change (Figure S4d).

Synthesis of Au(I), Pt(II), and Pd(II) Complexes. With the σ^3-P,N$_2$,S-hybrids **1S**, $\mathbf{2S}_{in}$, and $\mathbf{2S}_{out}$ in hand, we set out to examine their coordination behavior toward Au(I), Pt(II), and Pd(II) salts. As mentioned above, the symmetric hybrid **1S** exists as an equilibrium mixture of two conformers $\mathbf{1S}_{in}$ and $\mathbf{1S}_{out}$ at room temperature. Hence, both *in* and *out* type coordination modes are conceivable in the complexation reactions (Figure 6a; hereafter *in* and *out* are used to indicate the conformation of the σ^3-P,N$_2$,S-hybrids in metal complexes: *in* indicates $\mathbf{1S}_{in}$ or $\mathbf{2S}_{in}$, and *out* indicates $\mathbf{1S}_{out}$ or $\mathbf{2S}_{out}$). On the other hand, when the isolated asymmetric hybrids $\mathbf{2S}_{in}$ and $\mathbf{2S}_{out}$ are used as ligands, either *in* or *out* type coordination could be observed (Figure 6b). The structures of the metal complexes formed are summarized as simplified representations in Figure 7.

As shown in Table 3, **1S** (a mixture of $\mathbf{1S}_{in}$ and $\mathbf{1S}_{out}$) reacted with 1.1 equiv of AuCl(SMe$_2$) in toluene to give a mixture of the *in* type complex $\mathbf{11}_{in}$ and the *out* type complex $\mathbf{11}_{out}$. In solution, $\mathbf{11}_{out}$ was gradually converted to $\mathbf{11}_{in}$, indicating that $\mathbf{11}_{in}$ is thermodynamically more stable than $\mathbf{11}_{out}$. The conversion from $\mathbf{11}_{out}$ to $\mathbf{11}_{in}$ in toluene was almost complete within 1 h at room temperature. In contrast, $\mathbf{2S}_{in}$ and $\mathbf{2S}_{out}$ reacted with AuCl(SMe$_2$) to afford the *in* type complex $\mathbf{12}_{in}$ (eq 5) and the *out* type complex $\mathbf{12}_{out}$ (eq 6), respectively, with keeping the initial configuration at the phosphorus center. There was no sign of interconversion between $\mathbf{12}_{in}$ and $\mathbf{12}_{out}$ in CDCl$_3$ even after 10 h at room temperature. The *in* and *out* conformations of $\mathbf{11}_{in}$ and $\mathbf{12}_{out}$ were confirmed by X-ray crystallography (*vide infra*).

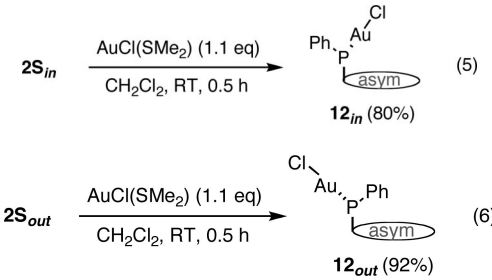

The complexation of the symmetric σ^3-P,N$_2$,S-hybrid **1S** with 0.5 equiv of PtCl$_2$ yielded three types of *trans*-Pt(II)-bis(phosphine) complexes, $\mathbf{13}_{i\text{-}i}$, $\mathbf{13}_{i\text{-}o}$, and $\mathbf{13}_{o\text{-}o}$ (Table 4), which are denoted as *in-in*,[16] *in-out*,[16] and *out-out* type, respectively. In refluxing toluene, the relative ratio of $\mathbf{13}_{i\text{-}i}/\mathbf{13}_{i\text{-}o}/\mathbf{13}_{o\text{-}o}$ changed from 4:54:42 (after 45 min) to 9:70:21 (after 2 h) and finally reached an equilibrium value of 90:10:~0[25] (after 4 days). Similarly, the complexation of **1S** with PdCl$_2$ afforded the *in-in* type and *in-out* type complexes $\mathbf{14}_{i\text{-}i}$ and $\mathbf{14}_{i\text{-}o}$ in a ratio of 92:8.[26] In this reaction, the *out-out* type complex $\mathbf{14}_{o\text{-}o}$ was not observed during the reaction. The same equilibrium states were attained by heating the isolated *in* type complexes $\mathbf{13}_{i\text{-}i}$ and $\mathbf{14}_{i\text{-}i}$ in refluxing toluene ($\mathbf{13}_{i\text{-}i}/\mathbf{13}_{i\text{-}o}/\mathbf{13}_{o\text{-}o}$ = 90:10:~0 after 4 days; $\mathbf{14}_{i\text{-}i}/\mathbf{14}_{i\text{-}o}/\mathbf{14}_{o\text{-}o}$= 92:8:~0 after 2 h). These results indicate that

(24) When dimethyl formamide-d_7 (DMF-d_7) was used as a guest, a similar downfield shift of the NH peaks was observed [$\Delta\delta$ = 0.08 ppm (10 equiv), 0.15 ppm (20 equiv)]. On the other hand, addition of tetrabutylammonium fluoride (10 equiv) or tetrabutylammonium chloride (10 equiv) to a solution of **1S** (12 mM in toluene-d_8 or CD$_2$Cl$_2$) did not cause appreciable downfield shift of the NH peaks.

(25) The preference for the *in* mode coordination was also found in a similar reaction in DMF (110 °C, 4 days: $\mathbf{13}_{i\text{-}i}/\mathbf{13}_{i\text{-}o}/\mathbf{13}_{o\text{-}o}$ = 92/8/~0).

(26) Owing to the poor solubility of PdCl$_2$ in toluene, a large amount (ca. 50%) of free ligand **1S** remained intact after 45 min.

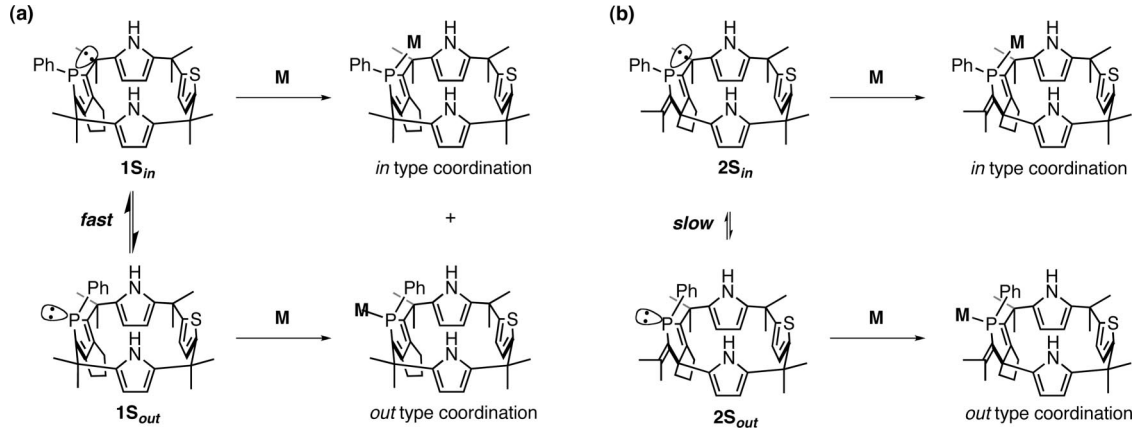

Figure 6. Coordination behavior of the symmetric hybrid **1S** (a) and asymmetric hybrids **2S**$_{in}$ and **2S**$_{out}$ (b).

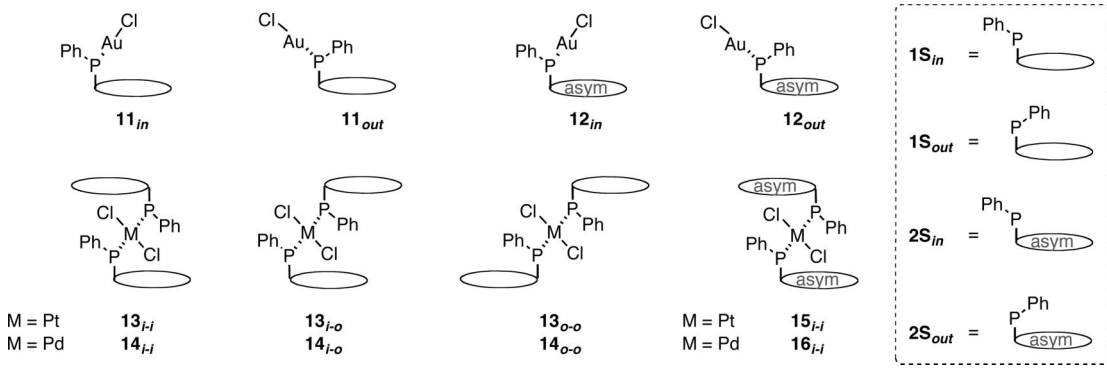

Figure 7. Simplified representations of the metal complexes.

Table 3. Reaction of 1S with AuCl(SMe$_2$)

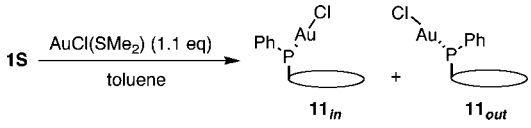

reaction conditions	relative ratio[a] **11**$_{in}$/**11**$_{out}$ (yield/%[b])
RT, 15 min	91:9 (80/−)
RT, 1 h	97:3 (86/−)
110 °C, 2 h	97:3 (84/−)

[a] Determined by ^{1}H NMR spectra. [b] Isolated yield.

the thermodynamic stability of **13** and **14** decreases in the order *in-in* > *in-out* ≫ *out-out*. It should be noted that, at room temperature, the interconversion among the *in-in*, *in-out*, and *out-out* complexes in $CDCl_3$ does not occur even after 10 h. The ^{31}P NMR spectra of **13**$_{i-i}$, **13**$_{i-o}$, and **13**$_{o-o}$ displayed characteristic peaks at δ 46.7 ppm ($^1J_{P-Pt}$ = 2476 Hz), δ 45.5 and 46.5 ppm ($^1J_{P-Pt}$ = 2400, 2560 Hz), and δ 45.7 ppm ($^1J_{P-Pt}$ = 2445 Hz), respectively. The observed ^{31}P−^{195}Pt coupling constants of 2400−2560 Hz are indicative of *trans* geometry of the two phosphine ligands for all complexes.[27] In the ^{31}P NMR spectrum of the Pd(II) complex **14**$_{i-i}$, a single peak was observed at δ 49.4 ppm. The structures of **13**$_{i-i}$, **13**$_{i-o}$, and **14**$_{i-i}$ were ultimately confirmed by X-ray crystallography (*vide infra*).

Finally, the reactions of the asymmetric σ^3-P,N$_2$,S-hybrid **2S**$_{in}$ with 0.5 equiv of MCl_2 (M = Pt, Pd) were examined (eq 7). In both cases, the *in-in* type *trans*-M(II)-bis(phosphine) complexes **15**$_{i-i}$, (M = Pt) and **16**$_{i-i}$ (M = Pd) were obtained as major products in 83% and 79% yield, respectively. The ^{31}P NMR spectra of **15**$_{i-i}$ and **16**$_{i-i}$ showed only one resonance at δ 40.2 ppm ($^1J_{P-P}$ = 2421 Hz) and δ 44.0 ppm, respectively, indicating that **15**$_{i-i}$ and **16**$_{i-i}$ had been isolated as single diastereomers. The X-ray diffraction analyses of **15**$_{i-i}$ and **16**$_{i-i}$ revealed that the two macrocyclic ligands have the same stereochemistry at the phosphorus and β-carbon atoms (*vide infra*), although the data of **15**$_{i-i}$ are not at the publishable level. The observed high diastereoselectivity represents that the asymmetric P,N$_2$,S-hybrid ligand **2S**$_{in}$ coordinated to the metal center discriminates the chirality of the second asymmetric ligand completely.

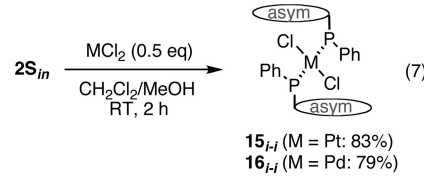

Crystal Structures of Au(I), Pt(II), and Pd(II) Complexes. The crystal structures of the Au(I) complexes **11**$_{in}$ (sym) and **12**$_{out}$ (asym), the Pt(II) complexes **13**$_{i-i}$ (sym) and **13**$_{i-o}$ (sym), and the Pd(II) complexes **14**$_{i-i}$ (sym) and **16**$_{i-i}$ (asym) were successfully elucidated by X-ray crystallography (Figures 8−12, and S5 (Supporting Information), Table S1). In the Au(I) complexes **11**$_{in}$ and **12**$_{out}$, the gold center adopts a linear geometry with P−Au−Cl bond angles of 173.20(2)−176.24(2)° (Figures 8 and 9). The Au−P and Au−Cl bond lengths [2.2391(8) and 2.2892(8) Å] of **11**$_{in}$ are close to the respective values of **12**$_{out}$ [2.2381(4) and 2.2871(4) Å] and those reported for the Au(I)-phosphole complexes.[28] In **11**$_{in}$, the Au−Cl moiety is located above the cavity provided by the symmetric σ^3-P,N$_2$,S macrocycle with a cone conformation. On the other hand, the Au−Cl moiety in **12**$_{out}$ is located outside the cavity provided

(27) (a) Rahn, J. A.; Baltusis, L.; Nelson, J. H. *Inorg. Chem.* **1990**, *29*, 750. (b) Power, W. P.; Wasylishen, R. E. *Inorg. Chem.* **1992**, *31*, 2176.

Table 4. Reaction of the Symmetric σ^3-P,N$_2$,S-Hybrid 1S with MCl$_2$ (M = Pt, Pd)

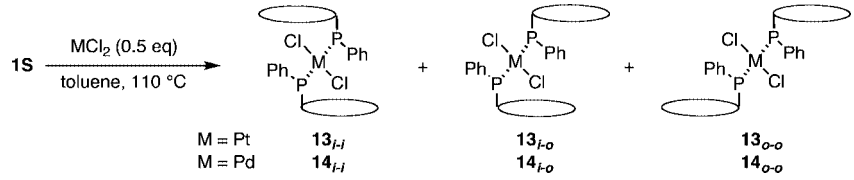

reaction time	relative ratio[a] (yield/%[b]) $\mathbf{13_{i\text{-}i}/13_{i\text{-}o}/13_{o\text{-}o}}$	$\mathbf{14_{i\text{-}i}/14_{i\text{-}o}/14_{o\text{-}o}}$
45 min	4:54:42 (−:49:37)	92: 8:∼0 (45:−:−)[c]
2 h	9:70:21 (12:60:24)	92: 8:∼0 (88:−:−)
4 days	90:10:∼0 (85:−:−)	

[a] Determined by ^{1}H NMR spectra. [b] Isolated yields. [c] About 50% of free ligand **1S** was recovered.

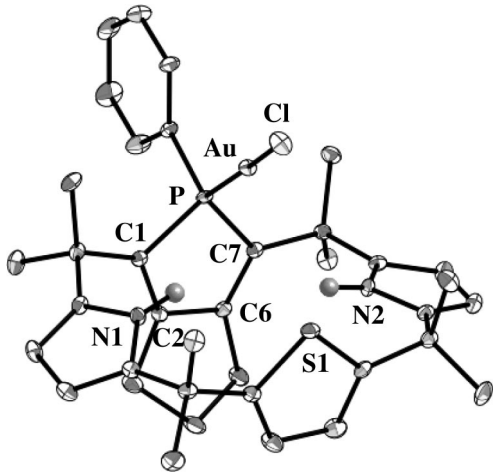

Figure 8. ORTEP diagram of $\mathbf{11}_{in}$ (30% probability ellipsoids). Hydrogen atoms are omitted for clarity. Selected bond lengths (Å) and angles (deg): Au−Cl, 2.2892(8); Au−P, 2.2391(8); C1−C2, 1.343(4); C2−C6, 1.469(4); C6−C7, 1.347(4); Cl−Au−P, 173.20(2).

by the asymmetric σ^3-P,N$_2$,S macrocycle with a partial cone conformation.

As shown in Figures 10−12 and S5, each metal center in the Pt(II) complexes $\mathbf{13}_{i\text{-}i}$ and $\mathbf{13}_{i\text{-}o}$ and the Pd(II) complexes $\mathbf{14}_{i\text{-}i}$ and $\mathbf{16}_{i\text{-}i}$ has a square-planar geometry, and two phosphorus atoms are coordinated in a *trans* orientation. The Pt−P and Pt−Cl bond lengths in $\mathbf{13}_{i\text{-}i}$ [2.3390(14), 2.3286(14) Å and 2.3035(12), 2.2992(11) Å] and $\mathbf{13}_{i\text{-}o}$ [2.3218(6), 2.3375(5) Å and 2.3195(5), 2.3018(6) Å] are close to the values reported for a *trans*-Pt(II)-bis(2,5-dialkylphosphole) complex [2.309(3), 2.318(3) Å and 2.296(3), 2.301(3) Å].[12g] Similarly, the Pd−P and Pd−Cl bond lengths of $\mathbf{14}_{i\text{-}i}$ [2.3496(8), 2.3548(8) Å and 2.2990(6), 2.3034(6) Å] and $\mathbf{16}_{i\text{-}i}$ [2.3488(10), 2.3343(8) Å and 2.2999(9), 2.3007(9) Å] are comparable to the values reported for a *trans*-Pd(II)-bis(2,5-dialkylphosphole)complex [2.325(7), 2.353(7) Å and 2.271(7), 2.280(7) Å].[12g]

In the *in-out* type Pt(II) complex $\mathbf{13}_{i\text{-}o}$, one of the symmetric σ^3-P,N$_2$,S ligands adopts a 1,2-alternate conformation and binds the platinum moiety outside the cavity, whereas the other adopts a cone conformation and binds the platinum moiety above the cavity. In the *in-in* type Pt(II) and Pd(II) complexes $\mathbf{13}_{i\text{-}i}$ and $\mathbf{14}_{i\text{-}i}$, the conformation of two symmetric σ^3-P,N$_2$,S ligands is basically the same as that of the *in* type ligand of $\mathbf{13}_{i\text{-}o}$. In these *in-in* type complexes, however, the whole structure has a C_{2h}

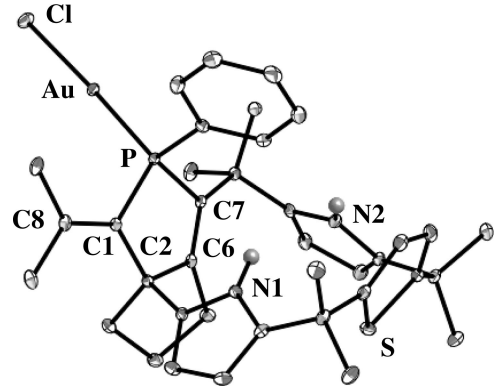

Figure 9. ORTEP diagram of $\mathbf{12}_{out}$ (30% probability ellipsoids). Hydrogen atoms are omitted for clarity. Selected bond lengths (Å) and angles (deg): Au−Cl, 2.2871(4); Au−P, 2.2381(4); C1−C2, 1.532(2); C1−C8, 1.343(3); C2−C6, 1.529(3); C6−C7, 1.343(3); Cl−Au−P, 176.24(2).

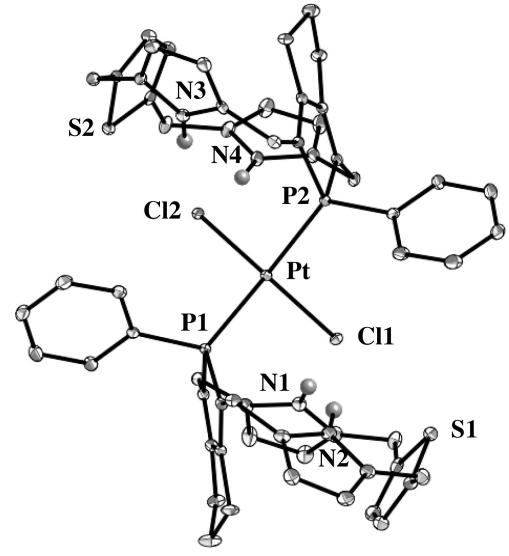

Figure 10. ORTEP diagram of $\mathbf{13}_{i\text{-}i}$ (30% probability ellipsoids). *meso*-Me groups and hydrogen atoms except for NH are omitted for clarity. Selected bond lengths (Å), angles (deg), and distances (Å): Pt−Cl1, 2.3035(12); Pt−Cl2, 2.2992(11); Pt−P1, 2.3390(14); Pt−P2, 2.3286(14); Cl1−Pt−P1, 94.76(4); Cl1−Pt−P2, 86.99(4); Cl2−Pt−P1, 86.57(4); Cl2−Pt−P2, 93.36(4); Cl1···N3, 3.27; Cl1···N4, 3.52; Cl2···N1, 3.50; Cl2···N2, 3.23.

(28) (a) Attar, S.; Bearden, W. H.; Alcock, N. W.; Alyea, E. C.; Nelson, J. H. *Inorg. Chem.* **1990**, *29*, 425. Au−P, 2.220(9)−2.227(2) Å; Au-Cl, 2.282(9)−2.288(2) Å. (b) Su, H.-C.; Fadhel, O.; Yang, C.-J.; Cho, T.-Y.; Fave, C.; Hissler, M.; Wu, C.-C.; Réau, R. *J. Am. Chem. Soc.* **2006**, *128*, 983. Au−P, 2.2290(16)−2.2300(16) Å; Au−Cl, 2.2638(18)−2.2895(19) Å (c) Dienes, Y.; Eggenstein, M.; Neumann, T.; Englert, U.; Baumgartner, T. *Dalton Trans.* **2006**, 1424. Au−P, 2.2249(12) Å; Au−Cl, 2.2946(12) Å.

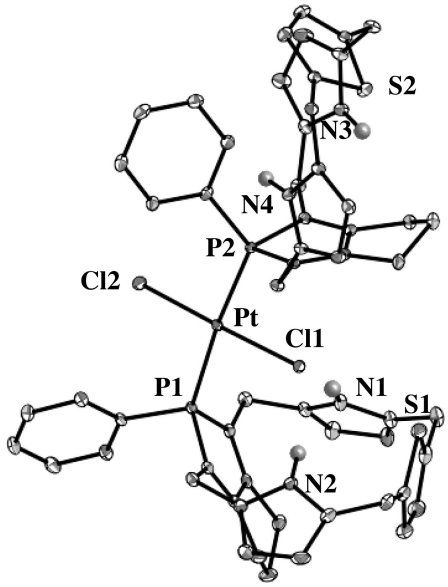

Figure 11. ORTEP diagram of **13**$_{i\text{-}o}$ (30% probability ellipsoids). *meso*-Me groups and hydrogen atoms except for NH are omitted for clarity. Selected bond lengths (Å), angles (deg), and distances (Å): Pt−Cl1, 2.3194(6); Pt−Cl2, 2.3018(6); Pt−P1, 2.3219(6); Pt−P2, 2.3375(6); Cl1−Pt−P1, 85.09 (2); Cl1−Pt−P2, 88.89(2); Cl2−Pt−P1, 93.20(2); Cl2−Pt−P2, 93.08(2); Cl1···N1, 3.41; Cl1···N2, 3.40.

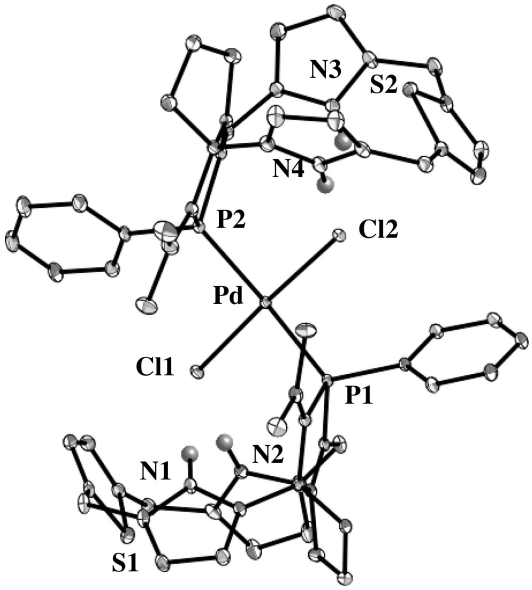

Figure 12. ORTEP diagram of **16**$_{i\text{-}i}$ (30% probability ellipsoids). *meso*-Me groups and hydrogen atoms except for NH are omitted for clarity. Selected bond lengths (Å), angles (deg), and distances (Å): Pd−Cl1, 2.2999(9); Pd−Cl2, 2.3007(9); Pd−P1, 2.3488(10); Pd−P2, 2.3343(8); Cl1−Pd−P1, 89.13(3); Cl1−Pd−P2, 93.01(3); Cl2−Pd−P1, 94.85(3); Cl2−Pd−P2, 86.04(3); Cl1···N1, 3.38; Cl1···N2, 3.18; Cl2···N3, 3.51; Cl2···N4, 3.23.

symmetry, and the metal center is located above the cavities of two macrocyclic ligands as though it is wrapped around. In the *in-in* type Pd(II) complex **16**$_{i\text{-}i}$, two asymmetric σ^3-P,N$_2$,S ligands coordinating to one palladium center have the same stereochemistry and adopt partial cone conformations. The coordination mode of **16**$_{i\text{-}i}$ is similar to those of **13**$_{i\text{-}i}$ and **14**$_{i\text{-}i}$.

Harvey and co-workers reported that the metal fragments of Rh(III) complexes of the upper-rim monophosphinated calix[4]arenes were located outside the cavity in the crystalline state.[14g,h] In sharp contrast, the crystal structures of the present complexes **11**$_{in}$, **13**$_{i\text{-}i}$, **13**$_{i\text{-}o}$, **14**$_{i\text{-}i}$, and **16**$_{i\text{-}i}$ clearly show that the symmetric and asymmetric σ^3-P,N$_2$,S-hybrids **1S** and **2S**$_{in}$ behave as monodentate P ligands to bind the metal above the cavity. This is attributable to the difference in rigidity at the phosphorus center between the monophosphinated calix[4]arenes and the σ^3-P,N$_2$,S-hybrids: the latter ligands are much more rigid than the former ones. Another interesting feature of the σ^3-P,N$_2$,S-hybrid ligands stems from the pyrrole units, which behave as hydrogen-bonding donors. In the ^{1}H NMR spectra of the Pt(II) and Pd(II) complexes **13**$_{i\text{-}i}$, **13**$_{i\text{-}o}$, **14**$_{i\text{-}i}$, **14**$_{i\text{-}o}$, **15**$_{i\text{-}i}$, and **16**$_{i\text{-}i}$ in $CDCl_3$, the NH resonances of the *in* type ligands were observed downfield relative to those of their free bases **1S**$_{in}$ and **2S**$_{in}$ ($\Delta\delta$ = 1.2−2.7 ppm; Table 5). In fact, in the crystal structures, two pyrrole rings of the *in* type macrocyclic ligands of **13**$_{i\text{-}i}$, **13**$_{i\text{-}o}$, **14**$_{i\text{-}i}$, and **16**$_{i\text{-}i}$ are tilted to direct the NH protons toward the chlorine atom bound to the metal with N···Cl distances of 3.18−3.52 Å, which are close to the reported values [3.264(7)−3.331(7) Å] of a chloride ion complex of *meso*-octamethylcalix[4]pyrrole.[3a] These observations demonstrate the presence of cooperative hydrogen-bonding interactions between the M−Cl (M = Pt, Pd) fragment and the NH protons in these complexes.

Concluding Remarks

Symmetric and asymmetric hybrid calixpyrroles containing a phosphole or a 2,3-dihydrophosphole unit (symmetric and asymmetric P,N$_2$,X-hybrids) were prepared for the first time via acid-promoted condensation reactions of the σ^4-phosphatripyrranes with 2,5-difunctionalized heteroles. As clearly revealed by X-ray crystallographic analyses of the σ^4-P,N$_2$,X-hybrids, the cavity size of the phosphole-containing hybrid calixpyrroles is tunable by exchanging the components of the macrocyclic backbone. The results on the complexation of the symmetric and asymmetric σ^3-P,N$_2$,S-hybrid calixpyrroles with Au(I), Pd(II), and Pt(II) salts represent that both the symmetric and asymmetric σ^3-P,N$_2$,S-hybrids behave as monodentate P ligands. It is of particular interest that the pyrrole NH protons can be utilized as hydrogen-bonding donors to the metal-bound chlorine atoms. The present study demonstrates the potential utility of the phosphole-containing hybrid calixpyrroles as a new class of multifunctional macrocyclic P ligands.

Experimental Section

General Comments. All melting points are uncorrected. ^{1}H, ^{13}C{^{1}H}, and ^{31}P{^{1}H} NMR spectra were recorded using $CDCl_3$ as the solvent unless otherwise noted. Chemical shifts are reported as the relative value versus tetramethylsilane (^{1}H and ^{13}C) and H_3PO_4 (^{31}P). MALDI-TOF and (HR-)FAB mass spectra were measured using CHCA and 3-nitrobenzyl alcohol as matrixes. CH_2Cl_2 and toluene were distilled from calcium hydride before use. All the reactions were performed under an argon or nitrogen atmosphere. Column chromatography was performed on silica gel or on a fast flow liquid chromatography system fitted with a silica gel column. Compound **3** was prepared by the reaction of the corresponding 2,5-diester with excess MeMgBr.[17] Other chemicals were of reagent grade quality, purchased commercially, and used without further purification unless otherwise noted. Although spectroscopic data clearly supported high purity of all the isolated compounds, we were not successful in obtaining satisfactory analytical data for **2S**$_{in}$, **2S**$_{out}$, **6**, **9O**, **10O**, **11**$_{in}$, **12**$_{in}$, **12**$_{out}$, **13**$_{i\text{-}o}$, **13**$_{o\text{-}o}$, **14**$_{i\text{-}i}$, **15**$_{i\text{-}i}$, and **16**$_{i\text{-}i}$ with an accuracy of ±0.4% probably due to incorporation of solvent molecules in the solid state. The ^{1}H

Table 5. N···Cl Distances and NH Resonances in the Pt(II) and Pd(II) Complexes

complex	N···Cl distances (Å)	NH resonances in $CDCl_3$ (ppm)	$\Delta\delta$ (ppm)[a]
13$_{i\text{-}i}$	3.23, 3.27, 3.50, 3.52	8.85	1.5−1.8
13$_{i\text{-}o}$	3.40[b], 3.41[b]	8.91[b], 7.19[c]	1.5−1.8[b], −0.2−0.1[c]
13$_{o\text{-}o}$		7.22	−0.2−0.1
14$_{i\text{-}i}$	3.26, 3.27, 3.49, 3.50	8.98	1.6−1.9
15$_{i\text{-}i}$		8.24, 9.34	1.2−1.4, 2.3−2.5
16$_{i\text{-}i}$	3.18, 3.23, 3.38, 3.51	8.37, 9.58	1.3−1.5, 2.6−2.7

[a] Differences in the NH resonances between the metal complexes (δ(M)) and the free ligands (δ(F)): $\Delta\delta = \delta(M) - \delta(F)$. [b] Values for the *in* type ligands. [c] Values for the *out* type ligands.

NMR spectra of these compounds are included as Figures S6−S18 in the Supporting Information.

Synthesis of Compounds 4, 5, and 6. To a solution of diol **3** (2.2 g, 6.3 mmol) in 60 mL (870 mmol) of pyrrole was added 0.78 mL (6.3 mmol) of $BF_3 \cdot OEt_2$. After stirring for 5 h at room temperature, CH_2Cl_2 (50 mL) and saturated $NaHCO_3$ solution (30 mL) were added. The water phase was extracted with CH_2Cl_2, and the organic extracts were combined, washed with brine, dried over Na_2SO_4, and evaporated. Purification by silica gel column chromatography (CH_2Cl_2/EtOAc = 50:1) followed by recrystallization from EtOAc/hexane afforded compounds **4** (890 mg, 32%; R_f = 0.6), **5** (740 mg, 26%; R_f = 0.5), and **6** (670 mg, 27%; R_f = 0.2) as colorless solids.

4: Mp 154−155 °C; ^{1}H NMR δ 1.38 (s, 6H), 1.41 (s, 6H), 1.54−1.62 (m, 1H), 1.90−1.94 (m, 1H), 2.09−2.25 (m, 4H), 5.88−5.90 (m, 2H), 5.99−6.01 (m, 2H), 6.70−6.71 (m, 2H), 7.48−7.59 (m, 3H), 7.97 (m, 2H), 9.12 (br s, 2H); ^{13}C{^{1}H} NMR δ 26.6, 26.6, 27.6, 27.7, 27.9, 28.1, 28.7, 28.8, 37.7, 37.8, 102.5, 106.4, 117.2, 128.8, 129.8, 131.7, 131.8, 135.0, 136.1, 138.3, 138.3, 158.0, 158.4; ^{31}P{^{1}H} NMR δ 69.3; MS (MALDI-TOF) *m*/*z* 447 (M^+). Anal. Calcd for $C_{27}H_{31}N_2PS$: C, 72.61; H, 7.00; N, 6.27; P, 6.94. Found: C, 72.60; H, 6.99; N, 6.27; P, 6.89.

5: Mp 163−164 °C; ^{1}H NMR δ 1.28 (s, 3H), 1.48 (s, 3H), 1.54 (d, 3H, J = 2.4 Hz), 1.65−1.71 (m, 1H), 1.68 (d, 3H, J = 2.0 Hz), 1.77−1.91 (m, 2H), 1.92−2.01 (m, 1H), 2.11−2.26 (m, 1H), 2.79−2.88 (m, 1H), 5.79−5.81 (m, 1H), 5.94−5.96 (m, 1H), 6.03−6.05 (m, 1H), 6.07−6.09 (m, 1H), 6.55−6.57 (m, 1H), 6.77−6.78 (m, 1H), 7−9 (br, 2H), 7.50−7.61 (m, 3H), 7.97 (br s, 1H), 9.60 (br s, 1H); ^{13}C{^{1}H} NMR δ 22.8, 22.9, 23.5, 23.5, 23.6, 23.8, 23.9, 27.6, 27.6, 30.1, 30.1, 34.6, 34.7, 38.2, 38.3, 60.0, 60.2, 102.8, 102.9, 104.8, 106.7, 106.9, 116.8, 118.5, 128.6, 131.5, 131.5, 132.3, 133.0, 133.1, 133.8, 134.1, 134.9, 139.8, 139.9, 147.5, 147.6, 168.6, 168.8; ^{31}P{^{1}H} NMR δ 62.2; MS (MALDI-TOF) *m*/*z* 447 (M^+). Anal. Calcd for $C_{27}H_{31}N_2PS$: C, 72.61; H, 7.00; N, 6.27. Found: C, 72.47; H, 6.99; N, 6.26.

6: Mp 180−182 °C; ^{1}H NMR δ 1.07 (s, 3H), 1.36 (s, 3H), 1.57 (d, 3H, J = 2.1 Hz), 1.69 (d, 3H, J = 1.5 Hz), 1.86−1.96 (m, 1H), 2.04−2.20 (m, 1H), 2.29−2.52 (m, 3H), 2.88−2.94 (m, 1H), 3.30 (s, 1H), 6.07−6.09 (m, 1H), 6.15−6.17 (m, 1H), 6.78−6.80 (m, 1H), 7.46−7.51 (m, 3H), 7.87−7.94 (m, 2H), 9.46 (br s, 1H); ^{13}C{^{1}H} NMR δ 22.6, 22.7, 23.7, 23.8, 23.9, 24.8, 24.9, 28.3, 33.1, 33.2, 34.4, 34.4, 60.6, 60.9, 72.8, 73.0, 104.8, 106.8, 118.8, 128.3, 128.5, 131.4, 131.4, 131.6, 131.8, 132.2, 133.1, 133.2, 133.2, 133.9, 134.4, 134.9, 148.4, 148.6, 163.2, 163.4; ^{31}P{^{1}H} NMR δ 62.4; MS (MALDI-TOF) *m*/*z* 397 (M^+).

Synthesis of Compounds 9S and 9O. Compounds **4** (50 mg, 0.11 mmol) and **8S** (22 mg, 0.11 mmol) were dissolved in CH_2Cl_2 (80 mL), and the solution was bubbled with N_2 for 40 min. $BF_3 \cdot OEt_2$ (0.014 mL, 0.11 mmol) was added to the solution, and the mixture was then stirred for 3.5 h at room temperature. The resulting mixture was washed with distilled water (3 × 80 mL), dried over Na_2SO_4, and evaporated to give a pale yellow solid, which was subjected to silica gel column chromatography (hexane/CH_2Cl_2 = 2:1) to give the σ^4-P,S,N_2-hybrid **9S** as a yellow solid (R_f = 0.4; 41 mg, 61%). A similar treatment of **4** with **8O** afforded the σ^4-P,N_2,O-hybrid **9O** as a yellow solid (R_f = 0.4; 39%).

9S: Mp 241−242 °C; ^{1}H NMR δ 1.27 (m, 1H), 1.32 (s, 6H), 1.36 (s, 6H), 1.65 (s, 6H), 1.72 (s, 6H), 1.86 (m, 1H), 2.10 (m, 4H), 5.79 (m, 4H), 6.78 (s, 2H), 7.50 (m, 3H), 7.90 (m, 2H), 9.09 (s, 2H); ^{13}C{^{1}H} NMR δ 26.7, 27.2, 28.0, 28.2, 31.4, 31.7, 37.4, 37.6, 38.1, 99.8, 101.7, 101.8, 123.6, 128.6, 129.1, 129.5, 131.8, 135.5, 136.5, 137.0, 141.3, 152.0, 158.4, 158.7; ^{31}P{^{1}H} NMR (toluene-d_8) δ 69.6; MS (FAB) *m*/*z* 610 (M^+); Anal. Calcd for $C_{37}H_{43}N_2PS_2$: C, 72.75; H, 7.10; N, 4.59; P, 5.07. Found: C, 72.85; H, 7.10; N, 4.47; P, 5.12.

9O: Mp 177−178 °C; ^{1}H NMR δ 1.27 (m, 1H), 1.39 (s, 6H), 1.40 (s, 6H), 1.60 (s, 6H), 1.67 (s, 6H), 1.82 (m, 1H), 2.11 (m, 4H), 5.76 (dd, 2H, J = 2.6, 2.6 Hz), 5.78 (dd, 2H, J = 2.6, 2.6 Hz), 6.05 (s, 2H), 7.51 (m, 3H), 7.96 (m, 2H), 9.57 (s, 2H); ^{13}C{^{1}H} NMR δ 22.6, 22.8, 23.3, 23.6, 23.7, 24.4, 24.6, 25.4, 25.7, 25.8, 25.9, 29.0, 29.2, 29.7, 29.8, 34.1, 36.0, 36.1, 37.6, 37.7, 60.2, 60.5, 100.2, 100.3, 100.9, 103.6, 103.8, 104.2, 130.1, 131.1, 131.2, 131.3, 133.5, 133.7, 134.4, 134.9, 137.9, 138.9, 139.2, 146.8, 147.0, 159.6, 159.7, 168.8, 169.0; ^{31}P{^{1}H} NMR δ 69.4; MS (MALDI-TOF) *m*/*z* 595 (M^+).

Synthesis of Compounds 10S and 10O. Compounds **5** (110 mg, 0.25 mmol) and **8S** (50 mg, 0.25 mmol) were dissolved in CH_2Cl_2 (300 mL), and $BF_3 \cdot OEt_2$ (0.014 mL, 0.11 mmol) was added to the solution. After stirring for 3.5 h at room temperature, the resulting mixture was washed with distilled water (3 × 150 mL), dried over Na_2SO_4, and evaporated. The products were subjected to silica gel column chromatography (hexane/CH_2Cl_2 = 2:1) to give the asymmetric σ^4-P,N_2,S-hybrid **10S** as a colorless solid (R_f = 0.3; 75 mg, 49%). A similar treatment of **5** with **8O** afforded the asymmetric σ^4-P,N_2,O-hybrid **10O** as a colorless solid (R_f = 0.3; 44%).

10S: Mp 252−253 °C; ^{1}H NMR δ 1.14 (s, 3H), 1.32 (s, 3H), 1.45 (d, 3H, J = 2.1 Hz), 1.64−1.75 (m, 17H), 1.80−2.02 (m, 1H), 2.10−2.26 (m, 1H), 2.40−2.55 (m, 1H), 2.73−2.79 (m, 1H), 5.63 (dd, 1H, J = 3.0, 3.0 Hz), 5.68 (dd, 1H, J = 3.0, 3.0 Hz), 5.82 (dd, 1H, J = 3.0, 3.0 Hz), 5.90 (dd, 1H, J = 3.0, 3.0 Hz), 6.85 (pseudo s, 2H), 7.26−7.60 (m, 4H), 7.84 (s, 1H), 8.40−8.52 (m, 1H), 8.93 (s, 1H); ^{13}C{^{1}H} NMR δ 22.7, 22.8, 22.9, 23.4, 23.5, 24.1, 24.2, 26.4, 26.5, 29.5, 30.0, 30.2, 30.4, 34.1, 34.2, 37.4, 37.6, 38.2, 38.3, 59.5, 59.9, 99.6, 100.4, 101.0, 103.4, 120.9, 121.3, 130.9, 131.4, 131.4, 131.9, 133.1, 133.3, 134.2, 134.2, 135.3, 139.7, 139.7, 141.2, 142.1, 147.0, 147.2, 153.7, 155.7, 168.7, 169.0; ^{31}P{^{1}H} NMR (toluene-d_8) δ 62.3; MS (MALDI-TOF) *m*/*z* 610 (M^+). Anal. Calcd for $C_{37}H_{43}N_2PS_2$: C, 72.75; H, 7.10; N, 4.59; P, 5.07. Found: C, 72.99; H, 7.14; N, 4.53; P, 5.37.

10O: Mp ca. 240 °C (dec); ^{1}H NMR δ 1.23 (s, 3H), 1.43 (s, 3H), 1.51 (d, 3H, J = 2.4 Hz), 1.61−1.79 (m, 17H), 1.89−1.99 (m, 1H), 2.12−2.26 (m, 1H), 2.48−2.56 (m, 1H), 2.77−2.82 (m, 1H), 5.63 (dd, 1H, J = 3.0, 3.0 Hz), 5.65 (dd, 1H, J = 3.0, 3.0 Hz), 5.75 (dd, 1H, J = 3.0, 3.0 Hz), 5.89 (dd, 1H, J = 3.0, 3.0 Hz), 6.04 (d, 1H, J = 2.8 Hz), 6.05 (d, 1H, J = 2.8 Hz), 7.3−7.7 (br, 4H), 8.4−8.7 (br, 1H), 9.00 (s, 1H), 9.32 (s, 1H); ^{13}C{^{1}H} NMR δ 22.6, 22.8, 23.3, 23.6, 23.7, 24.4, 24.6, 25.4, 25.7, 25.9, 25.9, 29.0, 29.2, 29.7, 29.8, 34.1, 36.0, 36.1, 37.6, 37.7, 60.2, 60.5, 100.2, 100.3, 100.5, 100.9, 103.6, 103.8, 104.2, 130.1, 131.1, 131.3, 131.3, 131.4, 133.5, 133.7, 134.4, 137.9, 138.9, 138.9, 139.2, 146.8,

14.70, 159.7, 159.7, 168.8, 169.0; $^{31}P\{^1H\}$ NMR δ 63.1; MS (MALDI-TOF) *m/z* 595 (M^+).

Synthesis of Compound 1X. To a degassed solution of **9S** (47 mg, 0.077 mmol) in toluene (5 mL) was added $P(NMe_2)_3$ (0.040 mL, 0.22 mmol), and the mixture was then stirred under reflux for 33 h. The resulting mixture was concentrated under reduced pressure and subjected to silica gel column chromatography (hexane/CH_2Cl_2 = 2:1) to give the symmetric σ^3-P,N,S-hybrid **1S** as a colorless solid (R_f = 0.5; 41 mg, 92%). A similar treatment of **9O** with $P(NMe_2)_3$ afforded the symmetric σ^3-P,N,O-hybrid **1O** as a colorless solid (R_f = 0.5; 72%).

1S: The ^1H NMR spectrum of **1S** indicated that, in toluene-d_8, two conformers are present in about 4:1 ratio. Major conformer: ^1H NMR (toluene-d_8) δ 1.39 (s, 6H), 1.46 (s, 6H), 1.61 (s, 6H), 1.63 (s, 6H), 1.7−2.3 (m, 6H), 5.95 (m, 2H), 5.96 (m, 2H), 6.63 (s, 2H), 6.9−7.1 (m, 3H), 7.34 (m, 2H), 7.43 (br s, 2H); $^{31}P\{^1H\}$ NMR (toluene-d_8) δ 32.1. Minor conformer: ^1H NMR (toluene-d_8) δ 1.30 (s, 6H), 1.57 (s, 6H), 1.58 (s, 6H), 1.61 (s, 6H), 1.7−2.3 (m, 6H), 5.79 (m, 2H), 5.88 (m, 2H), 6.60 (s, 2H), 6.9−7.1 (m, 3H), 7.34 (m, 4H); $^{31}P\{^1H\}$ NMR (toluene-d_8) δ 31.4; HR-FAB-MS calcd for $C_{37}H_{43}N_2PS$ (M^+) 578.2885, found 578.2896.

1O: The ^1H NMR spectrum of **1O** indicated that, in toluene-d_8, two conformers are present in about 5:1 ratio. Major conformer: ^1H NMR (toluene-d_8) δ 1.34 (s, 6H), 1.48 (s, 6H), 1.54 (s, 6H), 1.64 (s, 6H), 1.6−2.5 (m, 6H), 5.70 (m, 2H), 5.85 (m, 2H), 6.04 (s, 2H), 6.9−7.2 (m, 5H), 7.72 (br s, 2H); $^{31}P\{^1H\}$ NMR (toluene-d_8) δ 32.3. Minor conformer: ^1H NMR (toluene-d_8) δ 1.34 (s, 6H), 1.45 (s, 6H), 1.57 (s, 6H), 1.64 (s, 6H), 1.6−2.5 (m, 6H), 5.47 (m, 2H), 5.70 (m, 2H), 5.94 (s, 2H), 6.63 (br s, 2H), 6.9−7.2 (m, 5H); $^{31}P\{^1H\}$ NMR (toluene-d_8) δ 37.6; HR-FAB-MS calcd for $C_{37}H_{43}N_2PO$ (M^+) 562.3113, found 562.3099.

Synthesis of Compounds $2S_{in}$ and $2S_{out}$. To a degassed solution of **10S** (140 mg, 0.23 mmol) in toluene (20 mL) was added $P(NMe_2)_3$ (5.5 mL, 30 mmol), and the mixture was then stirred under reflux for 60 h. The resulting mixture was concentrated under reduced pressure and subjected to silica gel column chromatography (hexane/CH_2Cl_2 = 2:1) to give the asymmetric σ^3-P,N,S-hybrids $\mathbf{2S}_{out}$ (R_f = 0.4; 32 mg, 24%) and $\mathbf{2S}_{in}$ (R_f = 0.2; 80 mg, 60%) as a colorless solid, respectively.

$\mathbf{2S}_{in}$: Mp ca. 90 °C (dec); ^1H NMR δ 1.01 (s, 3H), 1.15−1.33 (m, 1H), 1.28 (s, 3H), 1.40 (s, 3H), 1.60−1.65 (m, 9H), 1.69 (s, 3H), 1.72 (s, 3H), 1.77−2.05 (m, 3H), 2.10−2.22 (m, 1H), 2.60−2.75 (m, 1H), 5.69 (dd, 1H, *J* = 3.0, 3.0 Hz), 5.75 (dd, 1H, *J* = 3.0, 3.0 Hz), 5.90−5.91 (m, 2H), 6.81 (d, 1H, *J* = 3.3 Hz), 6.83 (d, 1H, *J* = 3.3 Hz), 6.88 (br s, 1H), 7.03 (br s, 1H), 7.25−7.40 (m, 3H), 7.52−7.63 (m, 2H); $^{31}P\{^1H\}$ NMR δ 29.5; HR-FAB-MS calcd for $C_{37}H_{43}N_2PS$ (M^+) 578.2885, found 578.2894.

$\mathbf{2S}_{out}$: Mp ca. 70 °C (dec); ^1H NMR δ 1.19 (s, 3H), 1.20−1.30 (m, 1H), 1.53 (s, 3H), 1.58−1.67 (m, 10H), 1.71 (s, 3H), 1.75−1.90 (m, 2H), 1.81 (s, 3H), 1.93 (s, 3H), 1.99−2.07 (m, 1H), 2.45−2.52 (m, 1H), 5.71 (dd, 1H, *J* = 3.2, 3.2 Hz), 5.82−5.86 (m, 3H), 6.84 (pseudo s, 2H), 7−8 (br, 2H), 7.06 (br s, 1H), 7.21−7.35 (m, 4H); $^{31}P\{^1H\}$ NMR δ 17.7; HR-FAB-MS calcd for $C_{37}H_{43}N_2PS$ (M^+) 578.2885, found 578.2877. We were not successful in obtaining satisfactory ^{13}C NMR spectra of $\mathbf{2S}_{in}$ and $\mathbf{2S}_{out}$ because of the gradual interconversion between these two conformers in $CDCl_3$ solution during the prolonged measurement time.

Synthesis of Compounds 11_{in} and 11_{out}. To a Schlenk tube containing **1S** (57 mg, 0.099 mmol) and $AuCl(SMe_2)$ (32 mg, 0.11 mmol) was added 3 mL of toluene. After stirring for 1 h at room temperature, the resulting mixture was evaporated and subjected to silica gel column chromatography (hexane/CH_2Cl_2 = 2:1) to give $\mathbf{11}_{in}$ as a colorless solid (R_f = 0.5; 66 mg, 86%). When the reaction time was 15 min, a small amount of $\mathbf{11}_{out}$ (ca. 10%) was observed by ^1H and ^{31}P NMR spectra.

$\mathbf{11}_{in}$: Mp ca. 220 °C (dec); ^1H NMR δ 1.34 (s, 6H), 1.54 (s, 6H), 1.55−1.69 (m, 3H), 1.67 (s, 6H), 1.75 (s, 6H), 1.85−1.97 (m, 1H), 2.14−2.26 (m, 2H), 5.82 (dd, 2H, *J* = 3.2, 3.2 Hz), 5.87 (dd, 2H, *J* = 3.2, 3.2 Hz), 6.98 (s, 2H), 7.43−7.49 (m, 2H), 7.51−7.57 (m, 3H), 7.64−7.72 (m, 2H); $^{13}C\{^1H\}$ NMR δ 26.9, 26.9, 27.8, 27.9, 28.2, 28.2, 30.9, 31.5, 31.6, 31.8, 36.9, 37.1, 38.0, 100.1, 103.5, 103.5, 125.4, 125.9, 126.7, 129.5, 129.6, 132.5, 132.5, 133.4, 133.6, 135.4, 136.1, 137.3, 137.4, 140.8, 150.6, 161.6, 161.8; $^{31}P\{^1H\}$ NMR δ 53.8; HR-FAB-MS calcd for $C_{37}H_{43}N_2ClPSAu$ (M^+) 810.2239, found 810.2242.

$\mathbf{11}_{out}$: ^1H NMR δ 1.25 (s, 6H), 1.58 (s, 6H), 1.68 (s, 6H), 1.69 (s, 6H), 1.83−1.94 (m, 1H), 2.06−2.19 (m, 3H), 2.33−2.43 (m, 2H), 5.62 (dd, 2H, *J* = 3.0, 3.0 Hz), 5.76 (dd, 2H, *J* = 3.0, 3.0 Hz), 6.8−7.3 (br, 2H), 6.88 (s, 2H), 7.07 (br s, 2H), 7.30−7.33 (m, 2H), 7.42−7.46 (m, 1H); $^{31}P\{^1H\}$ NMR δ 52.1.

Synthesis of Compounds 12_{in} and 12_{out}. To a Schlenk tube containing $\mathbf{2S}_{in}$ (8 mg, 0.014 mmol) and $AuCl(SMe_2)$ (4.5 mg, 0.015 mmol) was added 1 mL of CH_2Cl_2. After stirring for 0.5 h at room temperature, the resulting mixture was evaporated and subjected to silica gel column chromatography (hexane/CH_2Cl_2 = 1:1) to give $\mathbf{12}_{in}$ as a pale yellow solid (R_f = 0.4; 9 mg, 80%). A similar treatment of $\mathbf{2S}_{out}$ with $AuCl(SMe_2)$ afforded the complex $\mathbf{12}_{out}$ as a colorless solid (R_f = 0.4; 92%).

$\mathbf{12}_{in}$: Mp ca. 240 °C (dec); ^1H NMR δ 1.13 (s, 3H), 1.24−1.39 (m, 1H), 1.43 (s, 3H), 1.55 (s, 3H), 1.65 (pseudo s, 6H), 1.69 (s, 3H), 1.70−1.92 (m, 2H), 1.77 (s, 3H), 1.81 (s, 3H), 2.02−2.18 (m, 1H), 2.28−2.37 (m, 1H), 2.77−2.82 (m, 1H), 5.70−5.72 (m, 2H), 5.88 (dd, 1H, *J* = 3.0, 3.0 Hz), 5.93 (dd, 1H, *J* = 3.0, 3.0 Hz), 6.97 (br s, 1H), 6.98 (d, 1H, *J* = 3.6 Hz), 7.15 (d, 1H, *J* = 3.6 Hz), 7.30 (br s, 1H), 7.4−8.3 (br, 2H), 7.46−7.56 (m, 3H); $^{13}C\{^1H\}$ NMR δ 22.5, 22.6, 23.8, 23.9, 26.5, 26.5, 26.6, 29.4, 29.7, 30.1, 30.5, 31.2, 31.3, 34.5, 37.2, 37.3, 38.4, 38.5, 62.7, 62.9, 99.6, 101.8, 102.9, 104.5, 122.5, 122.9, 128.4, 129.0, 129.2, 129.4, 129.9, 130.5, 131.3, 131.6, 131.6, 131.8, 132.3, 132.3, 138.2, 138.2, 141.0, 142.0, 148.4, 148.5, 153.2, 154.9, 168.4, 168.6; $^{31}P\{^1H\}$ NMR δ 48.8; HR-FAB-MS calcd for $C_{37}H_{43}N_2ClPSAu$ (M^+) 810.2239, found 810.2252.

$\mathbf{12}_{out}$: Mp 294−296 °C; ^1H NMR δ 1.20−1.37 (m, 1H), 1.28 (s, 3H), 1.58 (s, 3H), 1.63−1.75 (m, 10H), 1.78−1.93 (m, 2H), 1.85 (s, 3H), 1.89 (s, 3H), 2.03 (s, 3H), 2.18−2.32 (m, 1H), 2.55−2.65 (m, 1H), 5.80 (dd, 1H, *J* = 3.0, 3.0 Hz), 5.84 (dd, 1H, *J* = 3.0, 3.0 Hz), 5.87 (dd, 1H, *J* = 3.0, 3.0 Hz), 5.94 (dd, 1H, *J* = 3.0, 3.0 Hz), 6.73 (br s, 1H), 6.82 (d, 1H, *J* = 3.3 Hz), 6.88 (d, 1H, *J* = 3.3 Hz), 7.09 (br s, 1H), 7.43−7.48 (m, 2H), 7.52−7.64 (m, 3H); $^{13}C\{^1H\}$ NMR δ 23.4, 23.6, 23.8, 24.4, 24.5, 26.0, 26.2, 27.1, 29.5, 29.6, 30.5, 30.9, 32.2, 32.3, 35.4, 37.9, 38.1, 38.3, 38.3, 62.9, 63.1, 100.7, 103.2, 103.9, 103.9, 106.5, 121.1, 121.5, 127.0, 127.9, 129.4, 129.5, 129.8, 130.5, 131.9, 131.9, 132.3, 132.4, 133.1, 133.2, 133.4, 138.5, 138.5, 140.4, 140.6, 149.7, 149.9, 154.1, 154.5, 169.4, 169.6; $^{31}P\{^1H\}$ NMR δ 41.9; HR-FAB-MS calcd for $C_{37}H_{43}N_2ClPSAu$ (M^+) 810.2239, found 810.2240.

Synthesis of Compounds $13_{i\text{-}i}$, $13_{i\text{-}o}$, and $13_{o\text{-}o}$. To a Schlenk tube containing **1S** (20 mg, 0.034 mmol) and $PtCl_2$ (4.5 mg, 0.017 mmol) was added 2.0 mL of toluene, and the resulting mixture was heated under reflux for 2 h. The solution was evaporated and subjected to silica gel column chromatography (CH_2Cl_2/hexane = 2:1), affording the bisphosphine complexes $\mathbf{13}_{i\text{-}i}$ (R_f = 0.5; 3 mg, 12%), $\mathbf{13}_{i\text{-}o}$ (R_f = 0.3; 15 mg, 60%), and $\mathbf{13}_{o\text{-}o}$ (R_f = 0.2; 6 mg, 24%) as a pale yellow solid, respectively. When the reaction time was 4 days, complex $\mathbf{13}_{i\text{-}i}$ was obtained exclusively (85%); small amounts of $\mathbf{13}_{i\text{-}o}$ (ca. 10%) and $\mathbf{13}_{o\text{-}o}$ (trace) were also observed in the ^1H NMR spectrum of the crude products.

$\mathbf{13}_{i\text{-}i}$: Mp ca. 290 °C (dec); ^1H NMR δ 0.92−1.04 (m, 4H), 1.23 (s, 12H), 1.60−1.72 (m, 28H), 1.88−2.05 (m, 4H), 2.09 (s, 12H), 5.76−5.79 (m, 8H), 6.41 (s, 4H), 7.34−7.38 (m, 4H), 7.45−7.49 (m, 2H), 7.86−7.90 (m, 4H), 8.85 (s, 4H); $^{13}C\{^1H\}$ NMR δ 26.1, 26.8, 30.7, 31.5, 34.4, 37.8, 38.0, 38.1, 38.1, 99.4, 102.5, 124.7, 125.7, 125.9, 126.1, 128.2, 128.2, 128.3, 130.6, 132.8, 132.8, 132.9, 138.4, 138.7, 138.9, 141.6, 142.1, 150.6, 163.5, 163.6, 163.7;

$^{31}P\{^1H\}$ NMR δ 46.7 (J_{Pt-P} = 2476 Hz); HR-FAB-MS calcd for $C_{74}H_{86}N_4Cl_2P_2S_2Pt$ (M^+) 1421.4794, found 1421.4780. Anal. Calcd for $C_{74}H_{86}N_4Cl_2P_2S_2Pt$: C, 62.43; H, 6.09; N, 3.94. Found: C, 62.09; H, 6.38; N, 3.51.

13$_{i\text{-}o}$: Mp ca. 230 °C (dec); ^1H NMR δ 1.28 (s, 6H), 1.45 (s, 6H), 1.55−1.70 (m, 32H), 1.77−2.10 (m, 8H), 2.25 (s, 6H), 2.43−2.48 (m, 2H), 5.67 (dd, 2H, J = 3.0, 3.0 Hz), 5.80−5.82 (m, 6H), 6.55 (s, 2H), 6.84 (s, 2H), 7.19 (s, 2H), 7.35−7.46 (m, 6H), 7.53 (m, 2H), 7.92 (m, 2H), 8.91 (s, 2H); $^{13}C\{^1H\}$ NMR δ 14.1, 22.7, 25.7, 26.6, 26.7, 26.7, 26.9, 26.9, 27.4, 28.3, 28.3, 28.4, 29.0, 30.3, 30.4, 30.4, 30.5, 30.8, 31.3, 31.6, 31.6, 35.5, 35.5, 37.8, 37.9, 38.0, 38.4, 38.5, 38.6, 99.4, 101.5, 102.5, 103.1, 123.6, 124.4, 126.0, 126.7, 127.3, 127.9, 127.9, 128.0, 128.6, 128.7, 128.8, 130.3, 130.9, 132.8, 132.9, 132.9, 134.4, 134.5, 134.6, 138.1, 138.6, 138.8, 138.9, 139.0, 139.0, 139.2, 142.0, 142.1, 142.1, 142.2, 151.0, 152.2, 159.3, 159.4, 159.5, 163.2, 163.4, 163.5; $^{31}P\{^1H\}$ NMR δ 45.5 (J_{Pt-P} = 2400 Hz), 46.5 (J_{Pt-P} = 2560 Hz); HR-FAB-MS calcd for $C_{74}H_{86}N_4Cl_2P_2S_2Pt$ (M^+) 1421.4794; found 1421.4780.

13$_{o\text{-}o}$: Mp ca. 220 °C (dec); ^1H NMR δ 1.51 (s, 12H), 1.66 (s, 12H), 1.68 (s, 12H), 1.69 (s, 12H), 1.75−2.05 (m, 8H), 2.35−2.46 (m, 4H), 5.70 (dd, 4H, J = 3.0, 3.0 Hz), 5.79 (dd, 4H, J = 3.0, 3.0 Hz), 6.85 (s, 4H), 7.16−7.28 (m, 4H), 7.22 (br s, 4H), 7.31−7.35 (m, 2H), 7.54−7.59 (m, 4H); $^{13}C\{^1H\}$ NMR δ 27.4, 27.9, 28.0, 28.0, 28.7, 30.5, 30.7, 31.3, 37.9, 38.4, 38.5, 38.6, 101.2, 103.1, 123.8, 125.3, 125.6, 125.9, 128.4, 128.4, 128.5, 130.6, 134.5, 134.6, 134.7, 138.3, 138.7, 139.0, 139.2, 152.1, 159.6, 159.7, 159.8; $^{31}P\{^1H\}$ NMR δ 45.7 (J_{Pt-P} = 2445 Hz); HR-FAB-MS calcd for $C_{74}H_{86}N_4Cl_2P_2S_2Pt$ (M^+) 1421.4794, found 1421.4816.

Synthesis of Compound 14$_{i\text{-}i}$**.** To a Schlenk tube containing **1S** (10 mg, 0.017 mmol) and $PdCl_2$ (1.5 mg, 0.0085 mmol) was added 1.5 mL of toluene, and the resulting mixture was heated under reflux for 2 h. The solution was evaporated and subjected to silica gel column chromatography (hexane/CH_2Cl_2 = 2:1), affording the bisphosphine complex **14**$_{i\text{-}i}$ (R_f = 0.5; 10 mg, 88%) as a yellow solid.

14$_{i\text{-}i}$: Mp ca. 240 °C (dec); ^1H NMR δ 0.93−1.02 (m, 4H), 1.22 (s, 12H), 1.55−1.77 (m, 28H), 1.89−2.01 (m, 4H), 2.09 (s, 12H), 5.75−5.78 (m, 8H), 6.43 (s, 4H), 7.33−7.37 (m, 4H), 7.45−7.49 (m, 2H), 7.86−7.90 (m, 4H), 8.98 (s, 4H);$^{13}C\{^1H\}$ NMR δ 25.9, 26.7, 26.7, 26.8, 27.0, 30.6, 31.5, 35.1, 35.2, 35.2, 37.8, 38.0, 38.1, 38.2, 53.4, 99.4, 102.5, 124.8, 126.2, 126.5, 126.7, 128.2, 128.3, 128.4, 130.6, 133.0, 133.0, 133.1, 134.3, 139.9, 140.1, 140.4, 141.4, 142.2, 150.6, 162.9, 163.0, 163.1;$^{31}P\{^1H\}$ NMR δ 49.4; HR-FAB-MS calcd for $C_{74}H_{86}N_4Cl_2P_2S_2Pd$ (M^+) 1332.4181, found 1332.4198.

Synthesis of Compounds 15$_{i\text{-}i}$ **and 16**$_{i\text{-}i}$**.** To a suspension of $PtCl_2$ (2.3 mg, 0.0085 mmol) in MeOH (0.5 mL) was added a CH_2Cl_2(1 mL) solution of **2S**$_{in}$ (10 mg, 0.017 mmol). After stirring for 2 h at room temperature, the resulting mixture was evaporated. Purification with silica gel column chromatography (hexane/CH_2Cl_2 = 2:1) followed by recrystallization from CH_2Cl_2/MeOH gave **15**$_{i\text{-}i}$ as a pale yellow solid (R_f = 0.2; 10 mg, 83%). A similar treatment of **2S**$_{in}$ with $PdCl_2$ afforded the complex **16**$_{i\text{-}i}$ as a yellow solid (R_f = 0.2; 79%).

15$_{i\text{-}i}$: Mp ca. 220 °C (dec); ^1H NMR δ 0.85 (s, 6H), 1.10−1.30 (m, 2H), 1.36 (s, 6H), 1.54 (s, 6H), 1.59 (s, 6H), 1.62−1.79 (m, 4H), 1.69 (s, 6H), 1.88 (s, 6H), 1.93 (s, 6H), 1.95−2.13 (m, 4H), 2.07 (s, 6H), 2.69−2.75 (m, 2H), 5.66 (dd, 2H, J = 2.8, 2.8 Hz), 5.71 (dd, 2H, J = 2.8, 2.8 Hz), 5.80 (dd, 2H, J = 2.8, 2.8 Hz), 5.92 (dd, 2H, J = 2.8, 2.8 Hz), 6.03 (d, 2H, J = 3.6 Hz), 6.47 (d, 2H, J = 3.6 Hz), 7.45−7.57 (m, 6H), 7.87−7.93 (m, 4H), 8.24 (s, 2H), 9.34 (s, 2H); $^{13}C\{^1H\}$ NMR δ 22.4, 22.6, 22.6, 22.7, 23.0, 23.1, 26.1, 27.9, 28.0, 28.1, 28.8, 30.8, 30.9, 31.5, 33.0, 33.1, 33.2, 33.2, 37.7, 37.8, 37.9, 38.0, 38.3, 61.8, 62.0, 62.1, 99.7, 101.4, 101.8, 104.6, 121.6, 121.9, 127.6, 127.6, 127.7, 127.8, 128.2, 128.4, 128.7, 129.4, 129.8, 130.1, 130.3, 133.6, 134.5, 134.5, 134.6, 141.1, 141.1, 141.1, 141.3, 142.0, 150.5, 152.3, 155.6, 166.0, 166.1, 166.2; $^{31}P\{^1H\}$ NMR δ 40.2 (J_{Pt-P} = 2421 Hz); HR-FAB-MS calcd for $C_{74}H_{86}N_4Cl_2P_2S_2Pt$ (M^+) 1421.4794, found 1421.4819.

16$_{i\text{-}i}$: Mp ca. 220 °C (dec); ^1H NMR δ 0.86 (s, 6H), 1.10−1.25 (m, 2H), 1.35 (s, 6H), 1.54 (s, 6H), 1.60 (s, 6H), 1.62−1.79 (m, 4H), 1.70 (s, 6H), 1.86 (s, 6H), 1.91 (s, 6H), 1.95−2.13 (m, 4H), 2.06 (s, 6H), 2.68−2.74 (m, 2H), 5.67 (dd, 2H, J = 3.0, 3.0 Hz), 5.72 (dd, 2H, J = 3.0, 3.0 Hz), 5.81 (dd, 2H, J = 3.0, 3.0 Hz), 5.91 (dd, 2H, J = 3.0, 3.0 Hz), 6.05 (d, 2H, J = 3.6 Hz), 6.52 (d, 2H, J = 3.6 Hz), 7.45−7.57 (m, 6H), 7.85−7.91 (m, 4H), 8.37 (s, 2H), 9.58 (s, 2H); $^{13}C\{^1H\}$ NMR δ 22.5, 22.5, 22.6, 22.9, 23.0, 23.0, 26.1, 28.6, 28.6, 28.7, 28.8, 30.8, 31.1, 31.5, 33.0, 33.6, 33.6, 33.7, 37.7, 37.8, 37.9, 38.0, 38.3, 62.1, 62.2, 62.3, 99.7, 101.4, 101.9, 104.6, 121.7, 122.0, 127.6, 127.7, 127.8, 128.3, 128.6, 128.9, 129.2, 129.4, 129.6, 130.2, 130.8, 131.1, 131.4, 133.3, 134.6, 134.6, 134.7, 140.7, 140.8, 140.8, 141.4, 142.1, 150.3, 150.4, 150.6, 152.2, 155.7, 165.4, 165.5, 165.6; $^{31}P\{^1H\}$ NMR δ 44.0; HR-FAB-MS calcd for $C_{74}H_{86}N_4Cl_2P_2S_2Pd$ (M^+) 1332.4181, found 1332.4186.

X-ray Crystallography. Single crystals suitable for X-ray analyses were grown from CH_2Cl_2/MeOH (for **9S**, **9O**, **10S**, **12**$_{out}$, **13**$_{i\text{-}i}$, and **13**$_{i\text{-}o}$), CH_2Cl_2/hexane (for **10O**, **11**$_{in}$, and **14**$_{i\text{-}i}$), or CH_2Cl_2/MeCN (for **15**$_{i\text{-}i}$ and **16**$_{i\text{-}i}$). All X-ray crystallographic measurements were made on a Rigaku Saturn CCD area detector with graphite-monochromated Mo Kα radiation (0.71070 Å). The selected crystallographic data are summarized in Table S1. The structures were solved by using direct methods (SIR92[29] for **9O**, **11**$_{in}$, **13**$_{i\text{-}i}$, and **16**$_{i\text{-}i}$; SIR97[30] for **9S**, **10S**, **10O**, **13**$_{i\text{-}o}$, and **16**$_{i\text{-}o}$; SHELXS97[31] for **12**$_{out}$). Non-hydrogen atoms were refined anisotropically, and hydrogen atoms were refined using the rigid model. All calculations were performed using the CrystalStructure[32] crystallographic software package except for refinement, which was performed using SHELXL-97.[31] The crystals of **9S** consist of a pair of two independent molecules, one of which is depicted in Figure 2. The CIF files of **9S** and **9O** were uploaded as the Supporting Information files in ref 16.

Acknowledgment. This work was partially supported by Grants-in-Aid (Nos. 19027030 and 17350018) from the Ministry of Education, Culture, Sports, Science, and Technology of Japan. We thank Prof. Hidemitsu Uno (Ehime University) for his helpful suggestions about X-ray crystallographic analysis. T.N. acknowledges a JSPS fellowship for young scientists.

Supporting Information Available: ORTEP diagrams of **9O**, **10O**, and **14**$_{i\text{-}i}$ and CIF files for **10S**, **10O**, **11**$_{in}$, **12**$_{out}$, **13**$_{i\text{-}i}$, **13**$_{i\text{-}o}$, **14**$_{i\text{-}i}$, and **16**$_{i\text{-}i}$. This material is available free of charge via the Internet at http://pubs.acs.org.

OM800099H

(29) SIR92: Altomare, A.; Cascarano, G.; Giacovazzo, C.; Guagliardi, A.; Burla, M.; Polidori, G.; Camalli, M. *J. Appl. Crystallogr.* **1994**, *27*, 435.

(30) SIR97: Altomare, A.; Burla, M.; Camalli, M.; Cascarano, G.; Giacovazzo, C.; Guagliardi, A.; Moliterni, A.; Polidori, G.; Spagna, R. *J. Appl. Crystallogr.* **1999**, *32*, 115–119.

(31) Sheldrick, G. M. *SHELXL-97*; University of Göttingen: Germany, 1997.

(32) *CrystalStructure 3.8.0*: Crystal Structure Analysis Package; Rigaku and Rigaku/MSC: The Woodlands, TX, 2000−2006.